

COMPUTATION AND PROPERTIES OF THE EPSTEIN ZETA
FUNCTION WITH HIGH-PERFORMANCE IMPLEMENTATION
IN EPSTEINLIB

ANDREAS A. BUCHHEIT

Department of Mathematics, Saarland University, 66123 Saarbrücken, Germany

JONATHAN BUSSE

*Department of Mathematics, Saarland University, 66123 Saarbrücken, Germany
German Aerospace Center (DLR), 51147 Cologne, Germany*

RUBEN GUTENDORF

Department of Mathematics, Saarland University, 66123 Saarbrücken, Germany

ABSTRACT. The Epstein zeta function generalizes the Riemann zeta function to oscillatory lattice sums in higher dimensions. Beyond its numerous applications in pure mathematics, it has recently been identified as a key component in simulating exotic quantum materials. This work establishes the Epstein zeta function as a powerful tool in numerical analysis by rigorously investigating its analytical properties and enabling its efficient computation. Specifically, we derive a compact and computationally efficient representation of the Epstein zeta function and thoroughly examine its analytical properties across all arguments. Furthermore, we introduce a superexponentially convergent algorithm, complete with error bounds, for computing the Epstein zeta function in arbitrary dimensions. We also show that the Epstein zeta function can be decomposed into a power law singularity and an analytic function in the first Brillouin zone. This decomposition facilitates the rapid evaluation of integrals involving the Epstein zeta function and allows for efficient precomputations through interpolation techniques. We present the first high-performance implementation of the Epstein zeta function and its regularisation for arbitrary real arguments in EpsteinLib, a C library with Python and Mathematica bindings, and rigorously benchmark its precision and performance against known formulas, achieving full precision across the entire parameter range. Finally, we apply our library to the computation of quantum dispersion relations of three-dimensional spin materials with long-range interactions and Casimir energies in multidimensional geometries, uncovering higher-order corrections to known asymptotic formulas for the arising forces.

1. INTRODUCTION

The Epstein zeta function generalizes the Riemann zeta function to oscillatory lattice sums in higher dimensions. As introduced by Paul Epstein in 1903 [23, 24], the Epstein zeta function for a lattice $\Lambda = AZ^d$, $A \in \mathbb{R}^{d \times d}$ regular, and $\mathbf{x}, \mathbf{y} \in \mathbb{R}^d$, is defined as the meromorphic continuation of

$$Z_{\Lambda, \nu} \left| \begin{matrix} \mathbf{x} \\ \mathbf{y} \end{matrix} \right| = \sum'_{\mathbf{z} \in \Lambda} \frac{e^{-2\pi i \mathbf{y} \cdot \mathbf{z}}}{|\mathbf{z} - \mathbf{x}|^\nu}, \quad \operatorname{Re}(\nu) > d,$$

to $\nu \in \mathbb{C}$, where the primed sum excludes the summand where $\mathbf{z} = \mathbf{x}$. The Epstein zeta function has wide-ranging applications in pure and applied mathematics. It generalizes several special functions, such as the Dirichlet zeta and eta functions, as well as the Lerch zeta function. The non-trivial zeros of the Epstein zeta function have been extensively studied [42, 33]. The Epstein zeta function has recently been used to derive rigorous error bounds in boundary integral equations [50]. It forms a key ingredient of the Singular Euler–Maclaurin expansion (SEM), a recent generalization of the Euler–Maclaurin summation formula to singular functions in multi-dimensional lattices [8, 9].

The Epstein zeta function offers numerous applications in theoretical quantum physics and chemistry of technological relevance, especially in systems with long-range interactions. It describes lattice sums, such as Madelung constants, arising in theoretical chemistry [40, 21, 22]. It has been used in the recent prediction of new phases in unconventional superconductors with long-range interactions [10]. The Epstein zeta function appears in high-energy physics and quantum field theory in the computation of operator traces, relevant in the calculation of Casimir forces [3], and in the zeta regularisation of divergent path integrals [27]. An efficiently computable generalization of the Epstein zeta function to lattices with boundaries has recently been studied with direct applications to spin systems [7].

The numerical evaluation of the Epstein zeta function and its meromorphic continuation has been the topic of numerous studies. The first meromorphic continuation was constructed by Epstein using theta functions [23]. A major milestone in the computation of the Epstein zeta function was reached in the Chowla–Selberg formula [15], which allowed for the rapid evaluation of a particular Epstein zeta function in two dimensions. Terras derived an expansion of higher-dimensional zeta functions in terms of zeta functions of lower dimension [46]. Shanks provided a rapidly convergent representation of Epstein zeta functions for integer arguments [41]. A generalization of the Chowla–Selberg formula to higher dimensions was provided in [20]. These works relied on the computation of modified Bessel functions of the second kind and related integrals, which are restricted to special cases regarding the vectors \mathbf{x}, \mathbf{y} , and the lattice Λ . The modern algorithm for evaluating the Epstein zeta function is due to Crandall [16], whose representation offers superexponential convergence in the complete parameter range and relies exclusively upon the computation of incomplete gamma functions. A generalization of Crandall’s representation to point sets without translational invariance has recently been derived by one of the authors [7].

While Crandall’s work forms the basis for an algorithm to compute the Epstein zeta function, no library currently offers an implementation. This is due to numerous numerical challenges in its implementation. These challenges include instabilities in incomplete gamma function implementations for negative arguments, as well as

issues with the correct choice of truncation values and the treatment of numerical instabilities around singularities. Furthermore, the analytic properties of the Epstein zeta function in its arguments \mathbf{x} , \mathbf{y} are highly important [10], yet have not been rigorously studied.

This work solves the issues discussed above. We provide a compact and efficiently computable representation of the Epstein zeta function, based on Crandall's work, along with compact proofs. Using this representation, we offer the first rigorous discussion of the symmetries, singularities, and holomorphy of the Epstein zeta function in all its arguments. We isolate the singularities of the Epstein zeta function, writing it as a regularised analytic function and a power-law singularity, which allows both for the efficient evaluation of integrals and for exponentially convergent interpolations. We create an algorithm for computing the Epstein zeta function and its regularisation in any dimension, for any lattice, and for any choice of real arguments. We include a new algorithm and implementation of the incomplete gamma function, which is fast and offers full precision even for negative arguments. This algorithm is implemented in EpsteinLib, a first-of-its-kind high-performance C library for computing the Epstein zeta including both a Python and a Mathematica wrapper. We benchmark our method using numerous known formulas, obtaining full precision over the complete parameter range. Finally, we apply our method to the computation of quantum dispersion relations in spin systems and the evaluation of Casimir energies in quantum field theory.

This work is intended for a diverse audience with different interests and goals. We have, therefore, structured it as follows. In Section 2, we prove the efficiently computable representation and leverage it to derive the analytical properties of the Epstein zeta function. Section 3 discusses the numerical algorithm for its efficient and precise computation. We present the high-performance C library EpsteinLib and its usage in Section 4. The precision of our library is demonstrated in extensive numerical experiments against known formulas in Section 5. Section 6 showcases the application of our library to quantum spin wave dispersion relations and Casimir energies. We present our conclusions and an outlook in Section 7.

2. CRANDALL REPRESENTATION AND PROPERTIES OF THE EPSTEIN ZETA FUNCTION

2.1. Definition and elementary properties. We begin our exposition by introducing the concept of a d -dimensional lattice.

Definition 2.1 (Lattices). For $A \in \mathbb{R}^{d \times d}$ regular, we call the periodic set of points $\Lambda = A\mathbb{Z}^d$ a lattice. We denote by $E_\Lambda = A[-1/2, 1/2]^d$ the elementary lattice cell of Λ with volume $V_\Lambda = |\det A|$. We further define the reciprocal lattice $\Lambda^* = A^{-T}\mathbb{Z}^d$ with the elementary lattice cell $E_{\Lambda^*} = A^{-T}[-1/2, 1/2]^d$ of volume $V_{\Lambda^*} = 1/|\det A|$.

We then define the Epstein zeta function as follows.

Definition 2.2 (Epstein zeta function). Let Λ be a d -dimensional lattice, $\mathbf{x}, \mathbf{y} \in \mathbb{R}^d$ and $\nu \in \mathbb{C}$. The Epstein zeta function is defined as the meromorphic continuation of the lattice sum

$$Z_{\Lambda, \nu} \left| \begin{matrix} \mathbf{x} \\ \mathbf{y} \end{matrix} \right| = \sum'_{z \in \Lambda} \frac{e^{-2\pi i \mathbf{y} \cdot \mathbf{z}}}{|\mathbf{x} - \mathbf{z}|^\nu}, \quad \text{Re}(\nu) > d$$

to $\nu \in \mathbb{C}$.

The domain of definition for the meromorphic continuation is analyzed in detail in the next section in Theorem 2.13.

The Epstein zeta function exhibits numerous symmetries in its arguments \mathbf{x} and \mathbf{y} , as well as with respect to lattice rescaling, which we summarize in the following lemma.

Theorem 2.3 (Symmetries). *Let Λ be a d -dimensional lattice, let $\mathbf{x}, \mathbf{y} \in \mathbb{R}^d$, and let $\nu \in \mathbb{C}$ so that $\nu \neq d$ if $\mathbf{y} \in \Lambda^*$. Then:*

- (1) (Inversion symmetry) *Inversion of \mathbf{x} equals inversion of \mathbf{y} ,*

$$Z_{\Lambda, \nu} \left| \begin{array}{c} -\mathbf{x} \\ \mathbf{y} \end{array} \right| = Z_{\Lambda, \nu} \left| \begin{array}{c} \mathbf{x} \\ -\mathbf{y} \end{array} \right|, \text{ and } Z_{\Lambda, \nu} \left| \begin{array}{c} -\mathbf{x} \\ -\mathbf{y} \end{array} \right| = Z_{\Lambda, \nu} \left| \begin{array}{c} \mathbf{x} \\ \mathbf{y} \end{array} \right|.$$

- (2) (Translation symmetry) *The Epstein zeta function is, up to a prefactor, Λ -periodic in \mathbf{x} and Λ^* -periodic in \mathbf{y} . For $\mathbf{u} \in \Lambda$ and $\mathbf{v} \in \Lambda^*$, it holds that*

$$Z_{\Lambda, \nu} \left| \begin{array}{c} \mathbf{x} + \mathbf{u} \\ \mathbf{y} + \mathbf{v} \end{array} \right| = e^{-2\pi i \mathbf{y} \cdot \mathbf{u}} Z_{\Lambda, \nu} \left| \begin{array}{c} \mathbf{x} \\ \mathbf{y} \end{array} \right|.$$

- (3) (Scale symmetry) *For $s \in \mathbb{R} \setminus \{0\}$,*

$$Z_{\Lambda, \nu} \left| \begin{array}{c} \mathbf{x} \\ \mathbf{y} \end{array} \right| = |s|^\nu Z_{s\Lambda, \nu} \left| \begin{array}{c} s\mathbf{x} \\ \mathbf{y}/s \end{array} \right|.$$

Proof. We may restrict our discussion on $\text{Re}(\nu) > d$ by the uniqueness of the analytic continuation. There, the Epstein zeta function is defined via an absolutely convergent lattice sum, see Lemma A.1.

The first property is a direct consequence of $-\Lambda = \Lambda$. For the second, we write

$$Z_{\Lambda, \nu} \left| \begin{array}{c} \mathbf{x} + \mathbf{u} \\ \mathbf{y} + \mathbf{v} \end{array} \right| = e^{-2\pi i \mathbf{y} \cdot \mathbf{u}} \sum'_{\mathbf{z} \in \Lambda} e^{-2\pi i \mathbf{v} \cdot \mathbf{z}} \frac{e^{-2\pi i \mathbf{y} \cdot (\mathbf{z} - \mathbf{u})}}{|\mathbf{x} - (\mathbf{z} - \mathbf{u})|^\nu}.$$

The result follows from $\Lambda - \mathbf{u} = \Lambda$ and $e^{-2\pi i \mathbf{v} \cdot \mathbf{z}} = 1$ as $\mathbf{v} \cdot \mathbf{z} \in \mathbb{Z}$ for $\mathbf{z} \in \Lambda$ and $\mathbf{v} \in \Lambda^*$. Finally, scaling symmetry is obtained via

$$|s|^\nu Z_{s\Lambda, \nu} \left| \begin{array}{c} s\mathbf{x} \\ \mathbf{y}/s \end{array} \right| = \sum'_{\mathbf{z} \in \Lambda} |s|^\nu \frac{e^{-2\pi i \mathbf{y}/s \cdot s\mathbf{z}}}{|s\mathbf{z} - s\mathbf{x}|^\nu} = Z_{\Lambda, \nu} \left| \begin{array}{c} \mathbf{x} \\ \mathbf{y} \end{array} \right|. \quad \square$$

These symmetries can be effectively exploited to simplify computations involving generalized lattice sums. The scaling symmetry allows the reduction of general lattices to the case of unit elementary cell volume, $V_\Lambda = 1$. Further, the translation symmetry allows us to restrict all investigations to open neighborhoods of the elementary lattice cells $\mathbf{x} \in E_\Lambda$ and $\mathbf{y} \in E_\Lambda^*$. Translational symmetry allows for considering sums over multi-atomic lattices, where multiple particles with specific weights are arranged in the elementary lattice cell and Λ -periodically repeated in space.

Remark 2.4 (Multi-atomic lattices). Let Λ be a d -dimensional lattice, let $\mathbf{x}, \mathbf{y} \in \mathbb{R}^d$, and let $\nu \in \mathbb{C}$ so that $\nu \neq d$ if $\mathbf{y} \in \Lambda^*$. Consider $n \in \mathbb{N}_+$ particles at positions $\mathbf{d}_1, \dots, \mathbf{d}_n \in E_\Lambda$ with weights $g_1, \dots, g_n \in \mathbb{R}$. Then the holomorphic continuation of the multi-atomic lattice sum

$$S = \sum_{i=1}^n \sum'_{\mathbf{z} \in \Lambda + \mathbf{d}_i} g_i \frac{e^{-2\pi i \mathbf{y} \cdot \mathbf{z}}}{|\mathbf{x} - \mathbf{z}|^\nu}, \quad \text{Re}(\nu) > d$$

in ν is given in terms of the Epstein zeta function as

$$S = \sum_{i=1}^n g_i e^{-2\pi i \mathbf{y} \cdot \mathbf{d}_i} Z_{\Lambda, \nu} \left| \begin{array}{c} \mathbf{x} - \mathbf{d}_i \\ \mathbf{y} \end{array} \right|.$$

2.2. Computation of the Epstein zeta function and Crandall's representation. The defining lattice sum of the Epstein zeta function is only useful as a numerical tool for $\text{Re}(\nu) \gg d$, but the arising sum soon becomes numerically intractable as the real part of ν approaches the system dimension. It furthermore does not allow for insights into the holomorphic continuation in ν as well as into the properties of this function in its various parameters. In this section, we derive a representation that gives direct access to the holomorphic continuation of the Epstein zeta function in all parameters. The representation is based on works by Crandall [16] and [7] and serves both as the basis for our numerical algorithm and as a tool for proving the analytical properties of the Epstein zeta function. The following discussion focuses on the main proofs, while the proofs of technical lemmata are provided in Appendix B.

We start by defining the Fourier transform of integrable functions.

Definition 2.5 (Fourier transform). Let $f : \mathbb{R}^d \rightarrow \mathbb{C}$ be integrable. We define its Fourier transform $\mathcal{F}f = \hat{f}$ via

$$(\mathcal{F}f)(\mathbf{k}) = \int_{\mathbb{R}^d} f(\mathbf{x}) e^{-2\pi i \mathbf{k} \cdot \mathbf{x}} d\mathbf{x}, \quad \mathbf{k} \in \mathbb{R}^d.$$

The Poisson summation formula allows us to cast oscillatory sums over a lattice Λ in terms of sums of the Fourier transform of the summand function over the reciprocal lattice Λ^* .

Lemma 2.6 (Poisson summation formula). *Let $f : \mathbb{R}^d \rightarrow \mathbb{C}$ be a continuous integrable function. If there exist $C, \varepsilon > 0$ such that*

$$|f(\mathbf{z})| + |\hat{f}(\mathbf{z})| \leq C(1 + |\mathbf{z}|)^{-d-\varepsilon}, \quad \mathbf{z} \in \mathbb{R}^d,$$

then

$$V_{\Lambda} \sum_{\mathbf{z} \in \Lambda} f(\mathbf{z}) e^{-2\pi i \mathbf{z} \cdot \mathbf{y}} = \sum_{\mathbf{k} \in \Lambda^*} \hat{f}(\mathbf{k} + \mathbf{y}), \quad \mathbf{y} \in \mathbb{R}^d.$$

For a lattice $\Lambda = \mathbb{Z}^d$, the result is well-known, see [43, Corollary 2.6]. The case of general lattices is a slight generalization, shown for instance in [9, Lemma 3.2].

The incomplete gamma functions and their regularisation form key ingredients in the efficiently computable representation of the Epstein zeta function.

Remark 2.7. We denote by $\Gamma(s)$ the holomorphic extension of the gamma function to $s \in \mathbb{C} \setminus (-\mathbb{N}_0)$. For any $x \in \mathbb{C}$, $\text{Re}(x) > 0$, we denote by $\Gamma(s, x)$ the holomorphic extension of the upper incomplete Gamma function to $s \in \mathbb{C}$ and we denote by $\gamma(s, x)$ the holomorphic extension of the lower incomplete gamma function to $s \in \mathbb{C} \setminus (-\mathbb{N}_0)$ obeying the fundamental relation,

$$\Gamma(s) = \Gamma(s, x) + \gamma(s, x)$$

see Ref. [17, Section §8.2(ii)]. Tricomi's twice regularised lower incomplete gamma function $\gamma^*(s, x)$ is the holomorphic extension

$$\gamma^*(s, x) = \frac{\gamma(s, x)}{x^s \Gamma(s)}, \quad s, x > 0$$

to a jointly entire function in $(s, x) \in \mathbb{C} \times \mathbb{C}$, see Ref. [47].

The key idea for the Crandall representation is to decompose the function $|\cdot|^{-\nu}$ into a superexponentially decaying function that includes the singularity at $\mathbf{0}$ and a smooth function that includes the asymptotic power-law decay. We call these functions Crandall functions.

Definition 2.8 (Crandall functions). Let $\nu \in \mathbb{C}$ and $\mathbf{z} \in \mathbb{R}^d \setminus \{\mathbf{0}\}$. We define the upper Crandall function $G_\nu(\mathbf{z})$ as

$$G_\nu(\mathbf{z}) = \frac{\Gamma(\nu/2, \pi \mathbf{z}^2)}{(\pi \mathbf{z}^2)^{\nu/2}}, \quad G_\nu(\mathbf{0}) = -\frac{2}{\nu}.$$

Let $\nu \in \mathbb{C} \setminus (-2\mathbb{N}_0)$ and $\mathbf{z} \in \mathbb{C}^d$. Then, the lower Crandall function $g_\nu(\mathbf{z})$ is defined as

$$g_\nu(\mathbf{z}) = \Gamma(\nu/2) \gamma^*(\nu/2, \pi \mathbf{z}^2) = \frac{\gamma(\nu/2, \pi \mathbf{z}^2)}{(\pi \mathbf{z}^2)^{\nu/2}}.$$

The following lemma discusses the holomorphy of the Crandall functions in both arguments and provides bounds that describe their asymptotic decay as $|\mathbf{z}| \rightarrow \infty$.

Lemma 2.9 (Properties of Crandall functions). Let $\nu \in \mathbb{C}$ and $\mathbf{z} \in D$ with the complex sector

$$D = \{\mathbf{u} \in \mathbb{C}^d : |\operatorname{Re}(\mathbf{u})| > |\operatorname{Im}(\mathbf{u})|\},$$

where real and imaginary parts are applied component-wise and where $|\cdot|$ denotes the Euclidean norm.

- (1) (Holomorphy) The lower Crandall function $g_\nu(\mathbf{z})$ is jointly holomorphic in $(\nu, \mathbf{z}) \in \mathbb{C} \setminus (-2\mathbb{N}_0) \times \mathbb{C}^d$. The upper Crandall function $G_\nu(\mathbf{z})$ can be extended to a jointly holomorphic function in $(\nu, \mathbf{z}) \in \mathbb{C} \times D$. Finally, $G_\nu(\mathbf{0}) = -2/\nu$ is holomorphic in $\nu \in \mathbb{C} \setminus \{0\}$ with a simple pole at $\nu = 0$.
- (2) (Fundamental relation) For any $\lambda > 0$, it holds

$$(\mathbf{z}^2)^{-\nu/2} = \frac{(\lambda^2/\pi)^{-\nu/2}}{\Gamma(\nu/2)} \left(G_\nu(\mathbf{z}/\lambda) + g_\nu(\mathbf{z}/\lambda) \right).$$

Further, for $\operatorname{Re}(\nu) < 0$, we have $\lim_{\alpha \rightarrow 0^+} G_\nu(\alpha \mathbf{z}) = G_\nu(\mathbf{0}) = -2/\nu$. For all $\nu \in \mathbb{C}$, we have

$$\frac{1}{\Gamma(\nu/2)} (G_\nu(\mathbf{0}) + g_\nu(\mathbf{0})) = 0.$$

- (3) (Uniform bound) Define

$$u = \pi \operatorname{Re}(\mathbf{z}^2), \quad v = \max\{0, \operatorname{Re}(\nu/2) - 1\}.$$

We then have

$$|G_\nu(\mathbf{z})| \leq \frac{e^{-u}}{u - v}, \quad u > v.$$

Proof. (1) (Holomorphy) The lower Crandall function is the product of $\Gamma(\nu/2)$, which is holomorphic on $\mathbb{C} \setminus (-2\mathbb{N}_0)$, and the jointly entire function $(\nu, \mathbf{z}) \mapsto \gamma^*(\nu/2, \pi \mathbf{z}^2)$. Thus it is holomorphic on $(\nu, \mathbf{z}) \in (\mathbb{C} \setminus (-2\mathbb{N}_0)) \times \mathbb{C}^d$. For the upper Crandall function, first notice that $f(a, z) = \Gamma(a, z)/z^a$ is jointly holomorphic in $a \in \mathbb{C}$ and $z \in \mathbb{C}$ with $\operatorname{Re}(z) > 0$, which follows immediately from the representation [6, Eq. (2.1)],

$$f(a, z) = e^{-z} \int_0^\infty e^{-zt} (1+t)^{a-1} dt.$$

As $\mathbf{z} \in D$ is equivalent to $\operatorname{Re}(\mathbf{z}^2) > 0$, we have that

$$G_\nu(\mathbf{z}) = f(\nu/2, \pi\mathbf{z}^2)$$

is holomorphic on $(\nu, \mathbf{z}) \in \mathbb{C} \times D$.

(2) (Fundamental relation) The fundamental relation of the Crandall functions follows directly after inserting their definition from the associated relation of the incomplete Gamma functions in Remark 2.7. Furthermore, note that

$$\lim_{\alpha \rightarrow 0_+} f(a, \alpha z) = \int_0^\infty (1+t)^{a-1} dt = -1/a, \quad \operatorname{Re}(a) < 0.$$

Thus $G_\nu(\mathbf{z})$ can be continuously extended to $\mathbf{z} = \mathbf{0}$ and the limit coincides with the definition $G_\nu(\mathbf{0}) = -2/\nu$. Finally, for $\operatorname{Re}(\nu) < 0$, we have

$$\lim_{\alpha \rightarrow 0_+} ((\alpha\mathbf{z})^2)^{-\nu/2} = 0 = \frac{1}{\Gamma(\nu/2)} \left(G_\nu(\mathbf{0}) + g_\nu(\mathbf{0}) \right).$$

(3) (Uniform bound) Using the integral representation above, we find with $u = \operatorname{Re}(z)$ and $s = \operatorname{Re}(a)$,

$$|f(a, z)| \leq e^{-u} \int_0^\infty e^{-ut} (1+t)^{s-1} dt.$$

Following the proof of Theorem 2.1 in [6], we use the estimates $(1+t)^{s-1} \leq (e^t)^{s-1}$ for $s \geq 1$ and $(1+t)^{s-1} < 1$ for $s < 1$. Inserting them into the integral above yields

$$|f(a, z)| \leq e^{-u} \frac{1}{u - \max\{0, s-1\}}, \quad u > \max\{0, s-1\}.$$

We find the desired uniform bound after setting $a = \nu/2$ and $u = \pi\mathbf{z}^2$. \square

The Fourier transform connects the lower to the upper Crandall function.

Lemma 2.10. *Let $\operatorname{Re}(\nu) > d$ and $\lambda > 0$. Then*

$$\mathcal{F}(g_\nu(\cdot/\lambda))(\mathbf{k}) = \lambda^d G_{d-\nu}(\lambda\mathbf{k}), \quad \mathbf{k} \in \mathbb{R}^d.$$

Proof. We write the lower Crandall function in terms of its defining integral

$$g_\nu(\mathbf{z}/\lambda) = \left(\frac{\lambda^2}{\pi\mathbf{z}^2} \right)^{\nu/2} \int_0^{\pi\mathbf{z}^2/\lambda^2} t^{\nu/2} e^{-t} \frac{dt}{t},$$

see Ref. [2, Eq. (6.5.2)]. Substituting $t = \pi\mathbf{z}^2 s^2$ gives

$$g_\nu(\mathbf{z}/\lambda) = 2\lambda^\nu \int_0^{1/\lambda} s^\nu e^{-\pi\mathbf{z}^2 s^2} \frac{ds}{s}.$$

The Fourier transform now readily follows from $\mathcal{F}e^{-\pi(\cdot)^2/s^2} = s^{-d} e^{-\pi(\cdot)^2/s^2}$ and reads

$$(\mathcal{F}g_\nu(\cdot/\lambda))(\mathbf{k}) = 2\lambda^\nu \int_0^{1/\lambda} s^{\nu-d} e^{-\pi\mathbf{k}^2/s^2} \frac{ds}{s},$$

where the exchange of the integration order is justified due to the Fubini-Tonelli theorem, as the resulting integrand is absolutely integrable due to the restriction $\operatorname{Re}(\nu) > d$. For $\mathbf{k} = \mathbf{0}$, the integral evaluates to

$$\mathcal{F}(g_\nu)(\mathbf{0}) = -\lambda^d \frac{2}{d-\nu} = \lambda^d G_{d-\nu}(\mathbf{0}).$$

For $\mathbf{k} \neq \mathbf{0}$, we obtain the desired result after substituting $t = \pi \mathbf{k}^2 / s^2$,

$$\mathcal{F}(g_\nu)(\mathbf{k}) = \lambda^d (\pi \lambda^2 \mathbf{k}^2)^{-(d-\nu)/2} \int_{\pi \lambda^2 \mathbf{k}^2}^{\infty} t^{(d-\nu)/2} e^{-t} \frac{dt}{t} = \lambda^d G_{d-\nu}(\lambda \mathbf{k}). \quad \square$$

Crandall's representation now follows by rewriting the lattice sum for the Epstein zeta function in terms of the upper and lower Crandall functions. By applying the Poisson summation formula to the sum involving the lower Crandall functions, the Epstein zeta function is expressed in terms of two superexponentially convergent lattice sums, thus forming the basis for its efficient computation.

Theorem 2.11 (Crandall representation). *Let Λ be a d -dimensional lattice, let $\mathbf{x}, \mathbf{y} \in \mathbb{R}^d$, and let $\nu \in \mathbb{C}$ so that $\nu \neq d$ if $\mathbf{y} \in \Lambda^*$. Then the Epstein zeta function is well-defined and for any $\lambda > 0$, it holds that*

$$Z_{\Lambda, \nu} \left| \begin{array}{c} \mathbf{x} \\ \mathbf{y} \end{array} \right| = \frac{(\lambda^2/\pi)^{-\nu/2}}{\Gamma(\nu/2)} \left[\sum_{\mathbf{z} \in \Lambda} G_\nu \left(\frac{\mathbf{z} - \mathbf{x}}{\lambda} \right) e^{-2\pi i \mathbf{y} \cdot \mathbf{z}} + \frac{\lambda^d}{V_\Lambda} \sum_{\mathbf{k} \in \Lambda^*} G_{d-\nu}(\lambda(\mathbf{k} + \mathbf{y})) e^{-2\pi i \mathbf{x} \cdot (\mathbf{k} + \mathbf{y})} \right].$$

Proof. For the first part, we assume $\nu \in \mathbb{R}$ such that $\nu > d$. Then the defining lattice sum of the Epstein zeta function converges absolutely by Lemma A.1.

We then use the fundamental relation in Lemma 2.9 (2) to separate the power-law singularity into the upper and lower Crandall functions with a Riemann splitting parameter $\lambda > 0$. Inserting the result into the definition of the Epstein zeta function yields

$$Z_{\Lambda, \nu} \left| \begin{array}{c} \mathbf{x} \\ \mathbf{y} \end{array} \right| \frac{\Gamma(\nu/2)}{(\pi/\lambda^2)^{\nu/2}} = \sum_{\mathbf{z} \in \Lambda \setminus \{\mathbf{x}\}} G_\nu \left(\frac{\mathbf{z} - \mathbf{x}}{\lambda} \right) e^{-2\pi i \mathbf{y} \cdot \mathbf{z}} + \sum_{\mathbf{z} \in \Lambda \setminus \{\mathbf{x}\}} g_\nu \left(\frac{\mathbf{z} - \mathbf{x}}{\lambda} \right) e^{-2\pi i \mathbf{y} \cdot \mathbf{z}}.$$

Since $(G_\nu(\mathbf{0}) + g_\nu(\mathbf{0}))/\Gamma(\nu/2) = 0$, we can extend the summation to the whole lattice Λ in both sums without altering the result. The first sum already appears in Crandall's representation, whereas the second is brought to the desired form through Poisson summation. Note that g_ν is smooth by Definition 2.8 and decreases sufficiently fast for any choice of $\nu > d$ as a consequence of the fundamental relation Lemma 2.9 (2), because for positive real-valued ν , the Crandall functions are both non-negative. By Lemma 2.10, we have that $\mathcal{F}g_\nu(\cdot/\lambda) = \lambda^d G_{d-\nu}(\lambda \cdot)$, which is a continuous and superexponentially decreasing function by Lemma 2.9 (3). Thus, the requirements for Poisson summation hold, and the resulting sum reads

$$\frac{\lambda^d}{V_\Lambda} \sum_{\mathbf{k} \in \Lambda^*} G_{d-\nu}(\lambda(\mathbf{k} + \mathbf{y})) e^{-2\pi i \mathbf{x} \cdot (\mathbf{k} + \mathbf{y})},$$

obtaining the desired representation.

In Theorem 2.13, we show that the Crandall representation converges to a holomorphic function in $\nu \in \mathbb{C} \setminus \{d\}$ if $\mathbf{y} \in \Lambda^*$ and to an entire function in $\nu \in \mathbb{C}$

if $\mathbf{y} \in \mathbb{R}^d \setminus \Lambda^*$. By the identity theorem of holomorphic functions, this implies that Crandall's representation provides the unique holomorphic continuation of the Epstein zeta function. \square

The advantage of the Crandall representation over other ways to compute the Epstein zeta function is the superexponential decay of the function $G_\nu(\cdot)$. The resulting two lattice sums can be truncated to lattice points within a ball of radius $r > 0$ around \mathbf{x} and \mathbf{y} , as discussed in Section 3, yielding an efficiently computable representation.

2.3. Analytic properties. Crandall's representation not only serves as the basis for a numerical algorithm for computing the Epstein zeta function but also allows for a rigorous examination of its analytical properties across all arguments. A direct consequence is the functional equation of the Epstein zeta function.

Corollary 2.12 (Functional equation). *Let Λ be a d -dimensional lattice, let $\mathbf{x}, \mathbf{y} \in \mathbb{R}^d$, and let $\nu \in \mathbb{C}$ so that $\nu \neq d$ if $\mathbf{y} \in \Lambda^*$. The product*

$$\frac{(V_\Lambda^{2/d}/\pi)^{\nu/2}}{\Gamma((d-\nu)/2)} e^{\pi i \mathbf{x} \cdot \mathbf{y}} Z_{\Lambda, \nu} \left| \begin{array}{c} \mathbf{x} \\ \mathbf{y} \end{array} \right|$$

is then invariant under the parameter transformation

$$(\Lambda, \nu, \mathbf{x}, \mathbf{y}) \rightarrow (\Lambda^*, d - \nu, \mathbf{y}, -\mathbf{x}).$$

Proof. We start by inserting Crandall's representation for $\lambda = 1$ in the above formula. After exchanging the first and the second sum, we obtain

$$\begin{aligned} & \frac{V_\Lambda^{\nu/d}/V_{\Lambda^*}}{\Gamma((d-\nu)/2)\Gamma(\nu/2)} e^{\pi i \mathbf{x} \cdot \mathbf{y}} \sum_{\mathbf{k} \in \Lambda^*} G_{d-\nu}(\mathbf{k} + \mathbf{y}) e^{-2\pi i \mathbf{x} \cdot (\mathbf{k} + \mathbf{y})} \\ & + \frac{V_\Lambda^{\nu/d}}{\Gamma((d-\nu)/2)\Gamma(\nu/2)} e^{\pi i \mathbf{x} \cdot \mathbf{y}} \sum_{\mathbf{z} \in \Lambda} G_\nu(\mathbf{z} - \mathbf{x}) e^{-2\pi i \mathbf{y} \cdot \mathbf{z}}. \end{aligned}$$

After noticing that $V_\Lambda = 1/V_{\Lambda^*}$, swapping the indices \mathbf{k} and \mathbf{z} and using that $G_\nu(-\cdot) = G_\nu(\cdot)$, we have

$$\begin{aligned} & \frac{V_{\Lambda^*}^{(d-\nu)/d}}{\Gamma((d-\nu)/2)\Gamma(\nu/2)} e^{-\pi i \mathbf{x} \cdot \mathbf{y}} \sum_{\mathbf{z} \in \Lambda^*} G_{d-\nu}(\mathbf{z} - \mathbf{y}) e^{-2\pi i \mathbf{x} \cdot (-\mathbf{z} + \mathbf{y})} \\ & + \frac{V_{\Lambda^*}^{(d-\nu)/d}/V_{(\Lambda^*)^*}}{\Gamma((d-\nu)/2)\Gamma(\nu/2)} e^{-\pi i \mathbf{x} \cdot \mathbf{y}} \sum_{\mathbf{k} \in (\Lambda^*)^*} G_\nu(\mathbf{k} + (-\mathbf{x})) e^{-2\pi i \mathbf{y} \cdot \mathbf{k}}. \end{aligned}$$

The above expression is equal to Crandall's representation of the transformed product

$$\frac{(V_{\Lambda^*}^{2/d}/\pi)^{(d-\nu)/2}}{\Gamma(\nu/2)} e^{-\pi i \mathbf{x} \cdot \mathbf{y}} Z_{\Lambda^*, d-\nu} \left| \begin{array}{c} \mathbf{y} \\ -\mathbf{x} \end{array} \right|. \quad \square$$

The following theorem shows that the Epstein zeta function can be holomorphically extended not only in ν but also in \mathbf{x} and \mathbf{y} . This has several important consequences. First, it establishes the natural domain of definition for the Epstein zeta function with complex arguments \mathbf{x} , \mathbf{y} and ν . Since holomorphy implies smoothness, the theorem guarantees the existence of arbitrary higher-order derivatives of the Epstein zeta function with respect to its arguments. Finally, the domain of

holomorphy allows for a straightforward determination of the radius of convergence for Taylor series expansions in these arguments.

Theorem 2.13 (Holomorphy). *Let Λ be a d -dimensional lattice and $\nu \in \mathbb{C}$. We define the set $D \subseteq \mathbb{C}^d$ as the following intersection of d -dimensional complex cones with origins at $L \subseteq \mathbb{R}^d$,*

$$D_L = \{\mathbf{u} \in \mathbb{C}^d : |\operatorname{Re}(\mathbf{u}) - \mathbf{z}| > |\operatorname{Im}(\mathbf{u})| \ \forall \mathbf{z} \in L\}.$$

For $\mathbf{x} \notin \Lambda$, $\mathbf{y} \notin \Lambda^*$, the Epstein zeta function can be holomorphically extended to

$$(\nu, \mathbf{x}, \mathbf{y}) \in \mathbb{C} \times D_\Lambda \times D_{\Lambda^*}.$$

For $\mathbf{x} \in \Lambda$, $\mathbf{y} \notin \Lambda^*$, the Epstein zeta function can be holomorphically extended to

$$(\nu, \mathbf{y}) \in \mathbb{C} \times D_{\Lambda^*}$$

and for $\mathbf{y} \in \Lambda^*$, $\mathbf{x} \notin \Lambda$, the Epstein zeta function can be holomorphically extended to

$$(\nu, \mathbf{x}) \in (\mathbb{C} \setminus \{d\}) \times D_\Lambda$$

with a simple pole in $\nu = d$. Finally, for $\mathbf{x} \in \Lambda$ and $\mathbf{y} \in \Lambda^*$, the Epstein zeta function is holomorphic in $\nu \in \mathbb{C} \setminus \{d\}$ with a simple pole in $\nu = d$.

Proof. Consider the set $W = \mathbb{C} \times D_\Lambda \times D_{\Lambda^*}$. By Lemma 2.9, and Hartogs theorem [29, Theorem 2.2.8], each summand in Crandall's representation is jointly holomorphic in $(\nu, \mathbf{x}, \mathbf{y}) \in W$. We now need to show that holomorphy is preserved for the infinite lattice sums. For $r > 0$, we define $f_r : W \rightarrow \mathbb{C}$,

$$f_r(\nu, \mathbf{x}, \mathbf{y}) = \sum_{\substack{\mathbf{z} \in \Lambda \\ |\mathbf{z}| \leq r}} G_\nu \left(\frac{\mathbf{z} - \mathbf{x}}{\lambda} \right) e^{-2\pi i \mathbf{y} \cdot \mathbf{z}} + \frac{\lambda^d}{V_\Lambda} \sum_{\substack{\mathbf{k} \in \Lambda^* \\ |\mathbf{k}| \leq r}} G_{d-\nu}(\lambda(\mathbf{k} + \mathbf{y})) e^{-2\pi i \mathbf{x} \cdot (\mathbf{k} + \mathbf{y})},$$

which is holomorphic as the finite sum of holomorphic functions. We now show that $f_r \rightarrow f$ compact uniformly as $r \rightarrow \infty$ with $f : W \rightarrow \mathbb{C}$,

$$\frac{(\lambda^2/\pi)^{-\nu/2}}{\Gamma(\nu/2)} f(\nu, \mathbf{x}, \mathbf{y}) = Z_{\Lambda, \nu} \left| \begin{array}{c} \mathbf{x} \\ \mathbf{x} \end{array} \right|.$$

To this end, choose $\mathcal{K} \subset W$ compact. Using Lemma 2.9 (3), we can derive uniform bounds for the upper Crandall functions as follows

$$\left| G_\nu \left(\frac{\mathbf{z} - \mathbf{x}}{\lambda} \right) \right| \leq e^{-\pi \operatorname{Re}((\mathbf{z} - \mathbf{x})^2/\lambda^2)}, \quad \pi \operatorname{Re}((\mathbf{z} - \mathbf{x})^2/\lambda^2) > \max\{1, \operatorname{Re}(\nu/2)\}.$$

With

$$\operatorname{Re}((\mathbf{z} - \mathbf{x})^2) = (\mathbf{z} - \operatorname{Re}(\mathbf{x}))^2 - \operatorname{Im}(\mathbf{x})^2 \geq (|\mathbf{z}| - |\mathbf{x}|)^2 - |\mathbf{x}|^2 \geq |\mathbf{z}/2|^2$$

for all $\mathbf{z} \in \Lambda$ with $|\mathbf{z}| \geq 4 \sup_{\mathcal{K}} |\mathbf{x}|$, we find

$$\left| G_\nu \left(\frac{\mathbf{z} - \mathbf{x}}{\lambda} \right) \right| \leq e^{-\pi |\mathbf{z}/(2\lambda)|^2}, \quad \pi |\mathbf{z}/(2\lambda)|^2 > \sup_{\mathcal{K}} \max\{1, \operatorname{Re}(\nu/2)\}.$$

Similarly

$$|G_{d-\nu}(\lambda(\mathbf{k} + \mathbf{y}))| \leq e^{-\pi |\lambda \mathbf{k}/2|^2}, \quad \pi |\lambda \mathbf{k}/2|^2 > \sup_{\mathcal{K}} \max\{1, \operatorname{Re}((d-\nu)/2)\},$$

for all $\mathbf{k} \in \Lambda^*$ with $|\mathbf{k}| \geq 4 \sup_{\mathcal{K}} |\mathbf{y}|$. Finally, we have

$$\sup_{\mathcal{K}} |e^{-2\pi i \mathbf{y} \cdot \mathbf{z}}| \leq e^{c_1 |\mathbf{z}|}, \quad \sup_{\mathcal{K}} |e^{-2\pi i \mathbf{x} \cdot (\mathbf{k} + \mathbf{y})}| \leq c_2 e^{c_3 |\mathbf{k}|}.$$

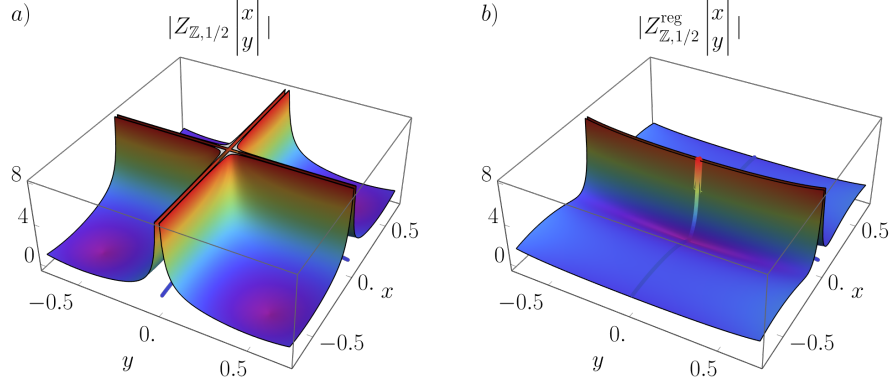


FIGURE 1. The one dimensional Epstein zeta function in $\nu = 1/2$ and $\Lambda = \mathbb{Z}$ admits discontinuities in the (reciprocal) lattice, in particular in $x = y = 0$ (a). The regularised Epstein zeta function in y is analytic in the Brillouin zone $-1/2 \leq y \leq 1/2$ and agrees with the Epstein zeta function in $y = 0$ (b).

For r chosen sufficiently large, such that the conditions for above bounds hold, we find

$$\sup_{\mathcal{K}} |f - f_r| \leq \sum_{\substack{\mathbf{z} \in \Lambda \\ |\mathbf{z}| > r}} e^{-\pi(\mathbf{z}/(2\lambda))^2} e^{c_1|\mathbf{z}|} + \frac{\lambda^d}{V_\Lambda} \sum_{\substack{\mathbf{k} \in \Lambda^* \\ |\mathbf{k}| > r}} e^{-\pi(\lambda\mathbf{k}/2)^2} c_2 e^{c_3|\mathbf{k}|} \rightarrow 0,$$

as $r \rightarrow \infty$. Convergence is obtained from Lemma A.1 using that the superexponential decay of the Gaussian dominates the exponential and that the resulting summand falls off faster than any power-law. From compact uniform convergence of $f_r \rightarrow f$ then follows holomorphy of f and thus of the Epstein zeta function on W , see [39, Theorem 10.28], which is a direct consequence of Morera's theorem.

Now consider the case $\mathbf{x} \in \Lambda$ and $\mathbf{y} \in D_{\Lambda^*}$. The proof then proceeds in analogy to before, where only the term $\mathbf{z} = \mathbf{x}$ in the first sum requires further attention. Recalling that $G_\nu(\mathbf{0}) = -2/\nu$, we find

$$\frac{(\lambda^2/\pi)^{-\nu/2}}{\Gamma(\nu/2)} G_\nu(\mathbf{0}) e^{-2\pi i \mathbf{y} \cdot \mathbf{z}} = -\frac{(\lambda^2/\pi)^{-\nu/2}}{\Gamma(\nu/2 + 1)} e^{-2\pi i \mathbf{y} \cdot \mathbf{z}},$$

as $1/\Gamma(s+1) = 1/(s\Gamma(s))$, for $s \in \mathbb{C}$. The apparent singularity at $\nu = 0$ is therefore removable. Thus the Epstein zeta function is holomorphic in $(\nu, \mathbf{y}) \in \mathbb{C} \times D_{\Lambda^*}$.

In case that $\mathbf{y} \in \Lambda^*$, we find that the term $\mathbf{k} = -\mathbf{y}$ is of the form

$$\frac{(\lambda^2/\pi)^{-\nu/2}}{\Gamma(\nu/2)} \frac{\lambda^d}{V_\Lambda} \frac{2}{\nu - d} e^{-2\pi i \mathbf{x} \cdot (\mathbf{k} + \mathbf{y})},$$

which exhibits a simple pole at $\nu = d$. Thus for $\mathbf{x} \in \Lambda$, the Epstein zeta function is holomorphic in $(\nu, \mathbf{y}) \in (\mathbb{C} \setminus \{d\}) \times D_{\Lambda^*}$. Finally, the discussion of the $\mathbf{z} = \mathbf{x}$ and $\mathbf{k} = -\mathbf{y}$ terms above also shows that for $\mathbf{x} \in \Lambda$ and $\mathbf{y} \in \Lambda^*$, the Epstein zeta function is holomorphic in $\nu \in \mathbb{C} \setminus \{d\}$ with a simple pole at $\nu = d$. \square

2.4. Singularities and regularization. The Epstein zeta function exhibits various singularities in its arguments. Understanding these singularities is of crucial importance in numerical applications that involve the Epstein zeta function as well as in physical applications. The singularities in \mathbf{x} can readily be deduced from the complex extension in \mathbf{x} of the summands of the defining lattice sum,

$$\frac{1}{((\mathbf{z} - \mathbf{x})^2)^{\nu/2}} \rightarrow \infty, \quad \mathbf{x} \rightarrow \mathbf{z},$$

for $\text{Re}(\nu) > 0$. The resulting summand function is holomorphic on the complex cone $D_{\{\mathbf{z}\}}$ centered at $\mathbf{z} \in \Lambda$. The singularities in \mathbf{x} correspond to singularities in the reciprocal lattice $\mathbf{y} \in \Lambda^*$ due to the functional equation. The singularity at $\mathbf{y} = \mathbf{0}$ is of particular interest in various applications of the Epstein zeta function, such as in anomalous quantum spin-wave dispersion relations, see Section 6.1, or in superconductors with long-range interactions, see Ref. [10]. For example, investigating the latter leads to singular integrals of the form

$$\int_{E_\Lambda^*} Z_{\Lambda, \nu} \left| \begin{array}{c} \mathbf{0} \\ \mathbf{y} \end{array} \right| f(\mathbf{y}) \, d\mathbf{y},$$

for some sufficiently regular function f . In order to evaluate the integral precisely, specialized quadrature rules are required that take into account the particular form of the singularity at $\mathbf{y} = \mathbf{0}$.

In this section, we show that the Epstein zeta function can be decomposed into a power-law singularity and a regularised function that is holomorphic around $\mathbf{y} = \mathbf{0}$. We further provide a modified Crandall representation that allows to compute the holomorphic part without cancellation error. The resulting regularised Epstein zeta function plays a key role in the recently discovered singular Euler–Maclaurin expansion [9], a generalization of the classical Euler–Maclaurin summation formula to higher dimensional lattice sums and physically relevant power-law singularities.

We define the regularised Epstein zeta function as follows.

Definition 2.14 (Regularised Epstein zeta function). Let Λ be a d -dimensional lattice, let $\mathbf{x} \in \mathbb{R}^d$, let $\mathbf{y} \in (\mathbb{R}^d \setminus \Lambda^*) \cup \{\mathbf{0}\}$ and let $\nu \in \mathbb{C}$. We define the regularised Epstein zeta function via

$$Z_{\Lambda, \nu}^{\text{reg}} \left| \begin{array}{c} \mathbf{x} \\ \mathbf{y} \end{array} \right| = e^{2\pi i \mathbf{x} \cdot \mathbf{y}} Z_{\Lambda, \nu} \left| \begin{array}{c} \mathbf{x} \\ \mathbf{y} \end{array} \right| - \frac{1}{V_\Lambda} \hat{s}_\nu(\mathbf{y}), \quad \mathbf{y} \neq \mathbf{0}$$

and continuously extended to $\mathbf{y} = \mathbf{0}$. Here \hat{s}_ν denotes the distributional Fourier transform of $s_\nu(\cdot) = |\cdot|^{-\nu}$ given by

$$\hat{s}_\nu(\mathbf{y}) = \frac{\pi^{\nu/2}}{\Gamma(\nu/2)} \Gamma((d - \nu)/2) (\pi \mathbf{y}^2)^{(\nu-d)/2}, \quad \nu \notin (d + 2\mathbb{N}_0).$$

For $\nu \in d + 2\mathbb{N}_0$, this Fourier transform is uniquely defined up to a polynomial of order $2k$, see [28]. We adopt the choice

$$\hat{s}_{d+2k}(\mathbf{y}) = \frac{\pi^{k+d/2}}{\Gamma(k+d/2)} \frac{(-1)^{k+1}}{k!} (\pi \mathbf{y}^2)^k \log(\pi \mathbf{y}^2), \quad k \in \mathbb{N}_0.$$

Crandall’s representation, which we modify for the regularised Epstein zeta function, enables its efficient computation without cancellation error.

Theorem 2.15 (Crandall representation for the regularised Epstein zeta function). *Let Λ be a d -dimensional lattice, let $\mathbf{x} \in \mathbb{R}^d$, let $\mathbf{y} \in (\mathbb{R}^d \setminus \Lambda^*) \cup \{\mathbf{0}\}$ and let $\nu \in \mathbb{C}$. Then for $\lambda > 0$,*

$$Z_{\Lambda, \nu}^{\text{reg}} \left| \begin{matrix} \mathbf{x} \\ \mathbf{y} \end{matrix} \right| = \frac{(\lambda^2/\pi)^{-\nu/2}}{\Gamma(\nu/2)} \left[\sum_{\mathbf{z} \in \Lambda} G_{\nu} \left(\frac{\mathbf{z} - \mathbf{x}}{\lambda} \right) e^{-2\pi i \mathbf{y} \cdot (\mathbf{z} - \mathbf{x})} \right. \\ \left. + \frac{\lambda^d}{V_{\Lambda}} \left[G_{d-\nu, \lambda}^{\text{reg}}(\mathbf{y}) + \sum_{\substack{\mathbf{k} \in \Lambda^* \\ \mathbf{k} \neq \mathbf{0}}} G_{d-\nu}(\lambda(\mathbf{k} + \mathbf{y})) e^{-2\pi i \mathbf{x} \cdot \mathbf{k}} \right] \right]$$

where the regularised upper Crandall function is defined as

$$G_{\nu, \lambda}^{\text{reg}}(\mathbf{y}) = G_{\nu}(\lambda \mathbf{y}) - \lambda^{-\nu} \pi^{-(d-\nu)/2} \Gamma((d-\nu)/2) \hat{s}_{d-\nu}(\mathbf{y}).$$

If $\nu \notin -2\mathbb{N}_0$, we have

$$G_{\nu, \lambda}^{\text{reg}}(\mathbf{y}) = -g_{\nu}(\lambda \mathbf{y})$$

and if $\nu = -2k$ for $k \in \mathbb{N}_0$ it holds that

$$G_{\nu, \lambda}^{\text{reg}}(\mathbf{y}) = \frac{(-1)^k}{k!} (H_k - \gamma - \lambda^{2k} \log \lambda^2) (\pi \mathbf{y}^2)^k - \sum_{\substack{n=0 \\ n \neq k}}^{\infty} \frac{(-\pi \mathbf{y}^2)^n}{(n-k)n!}.$$

Here γ is the Euler–Mascheroni constant, $H_0 = 0$ and H_n is the n -th harmonic number for $n \in \mathbb{N}_+$.

Proof. We rewrite the regularised Epstein zeta by subtracting the singularity from the $\mathbf{k} = \mathbf{0}$ summand in the second sum of Crandall’s representation. For $d - \nu \notin (-2\mathbb{N}_0)$,

$$G_{d-\nu, \lambda}^{\text{reg}}(\mathbf{y}) = G_{d-\nu}(\lambda \mathbf{y}) - \frac{\Gamma((d-\nu)/2)}{(\pi \lambda^2 \mathbf{y}^2)^{(d-\nu)/2}}$$

is given in terms of the lower Crandall function by the fundamental relation [2, Eq. (6.5.3)]. If $d - \nu = -2k$ for some $k \in \mathbb{N}_0$, the representation for

$$G_{d-\nu, \lambda}^{\text{reg}}(\mathbf{y}) = (\pi \lambda^2 \mathbf{y}^2)^k \left(\Gamma(-k, \pi \lambda^2 \mathbf{y}^2) + \frac{(-1)^k}{k!} (\log(\pi \lambda^2 \mathbf{y}^2) - \log \lambda^2) \right)$$

is obtained, by applying the series representation [2, Eq. (5.1.12)]

$$\Gamma(-k, z) = \frac{(-1)^k}{k!} (H_k - \ln z) - \sum_{\substack{n=0 \\ n \neq k}}^{\infty} \frac{(-z)^n}{(n-k)k!}$$

see Ref. [2, Eq. (5.1.12)] at $z = \pi \lambda^2 \mathbf{y}^2$. \square

By this representation, the regularised Epstein zeta function can be holomorphically extended in \mathbf{y} around $\mathbf{0}$.

Theorem 2.16 (Holomorphy of the regularised Epstein zeta function). *Let Λ be a d -dimensional lattice. Then the regularised Epstein zeta function can be holomorphically extended to*

$$(\nu, \mathbf{x}, \mathbf{y}) \in (\mathbb{C} \setminus (d + 2\mathbb{N}_0)) \times D_{\Lambda} \times D_{\Lambda^* \setminus \{\mathbf{0}\}}.$$

For $\nu \in (d + 2\mathbb{N}_0)$, the regularised Epstein zeta function is holomorphic in

$$(\mathbf{x}, \mathbf{y}) \in D_{\Lambda} \times D_{\Lambda^* \setminus \{\mathbf{0}\}}.$$

Finally, for $\mathbf{x} \in \Lambda$, the regularized Epstein zeta function is holomorphic on

$$(\nu, \mathbf{y}) \in (\mathbb{C} \setminus (d + 2\mathbb{N}_0)) \times D_{\Lambda^* \setminus \{\mathbf{0}\}}.$$

Proof. In proof of Theorem 2.13, we have shown holomorphy of every summand in Crandall's representation as well as compact uniform convergence. Thus, the domain of holomorphy of the Epstein zeta function corresponds to the intersection of the domains of holomorphy of all summands.

Removing the $\mathbf{k} = \mathbf{0}$ summand $G_{d-\nu}(\lambda(\mathbf{0} + \mathbf{y}))$ in the second sum in Crandall's representation extends holomorphy in \mathbf{y} to $D_{\Lambda^* \setminus \{\mathbf{0}\}}$ and removes the potential pole at $\nu = d$ in case that $\mathbf{y} = \mathbf{0}$. The regularised Epstein zeta function is then obtained by adding the regularised Crandall function $G_{d-\nu, \lambda}^{\text{reg}}(\mathbf{y})$, which is holomorphic in

$$(\nu, \mathbf{y}) \in (\mathbb{C} \setminus (-2\mathbb{N}_0)) \times \mathbb{C}^d,$$

where the exclusions in ν are due to the poles of the gamma function. In case that $\nu \in (d + 2\mathbb{N}_0)$, the resulting summand is entire in $\mathbf{y} \in \mathbb{C}^d$ by Lemma B.3. The intersection of the domains of analyticity then yields the desired result. \square

The holomorphy of the regularised Epstein zeta function in an open complex neighborhood of the Brillouin in \mathbf{y} leads to exponential convergence of an interpolating polynomial in the number of interpolants of an interpolating function [4]. Adding the singularity then allows for the near-instant evaluation of the Epstein zeta function.

3. ALGORITHM

In this section, we present an algorithm for efficiently computing the Epstein zeta for arbitrary real parameters. While Crandall's representation forms the basis for computing the Epstein zeta function in terms of a sum over superexponentially decaying function values, many numerical challenges remain. In this chapter, we present Algorithm 1, which evaluates the Epstein zeta function for arbitrary real parameters to full precision for dimensions $d \leq 10$. The discussion of the algorithm is structured as follows. The preprocessing of the parameters, especially the projection of the vectors to the elementary lattice cell, is discussed in Section 3.1. Near poles and zeros of the gamma and Crandall functions, explicit evaluations of the Epstein zeta function as discussed in Section 3.2 are needed to guarantee a stable evaluation. In Section 3.3, our choice of the summation cutoff is justified and techniques for reducing roundoff errors are discussed. Finally, we outline the computation of the upper incomplete gamma function in Section 3.4.

3.1. Preprocessing. Whenever possible, both sums in Crandall's representation should decay similarly fast, to ensure a low number of total summands to evaluate. To that end, we rescale the lattice matrix as in Theorem 2.3 so that its determinant equals one. By translational symmetry, we restrict the evaluation to vectors \mathbf{x}, \mathbf{y} in their respective elementary lattice cells. The following statement allows for the projection of \mathbf{x} to its elementary lattice cell as in the second step of our algorithm.

Lemma 3.1. *Let $\Lambda = AZ^d$ for $A \in \mathbb{R}^{d \times d}$ regular, let $\mathbf{x} \in \mathbb{R}^d$ and*

$$\mathbf{v} = A \lfloor A^{-1} \mathbf{x} + \mathbf{1}/2 \rfloor$$

where $\mathbf{1} = (1, \dots, 1)^T \in \mathbb{R}^d$ is the one-vector and $\lfloor \cdot \rfloor$ is the element-wise applied floor function. Then $\mathbf{v} \in \Lambda$ and $\mathbf{x} - \mathbf{v} \in E_\Lambda$.

Algorithm 1: Computation of the Epstein zeta function.

Input: $d \in \mathbb{N}$, $A \in \mathbb{R}^{d \times d}$ regular, $\mathbf{x}, \mathbf{y} \in \mathbb{R}^d$, $\nu \in \mathbb{R}$

1. **Rescale lattice matrix and vectors**
 $a = V_\Lambda^{1/d}$, $A \leftarrow A/a$, $\mathbf{x} \leftarrow \mathbf{x}/a$, $\mathbf{y} \leftarrow a\mathbf{y}$
2. **Project \mathbf{x} and \mathbf{y} to elementary lattice cells**
 $\mathbf{x}' = A^{-1}\mathbf{x}$, $\mathbf{y}' = A^T\mathbf{y}$
for $i = 1, \dots, d$ **do**
 $\quad \lfloor x'_i \leftarrow ((x'_i + 1/2) \bmod 1) - 1/2$
 $\quad \lfloor y'_i \leftarrow ((y'_i + 1/2) \bmod 1) - 1/2$
 $\mathbf{x}' \leftarrow A\mathbf{x}'$, $\mathbf{y}' \leftarrow A^{-T}\mathbf{y}'$
3. **Handle special cases**
if $\nu = d \wedge \mathbf{y}' = 0 \wedge \text{regularised} = \text{False}$ **then**
 $\quad \lfloor$ **return** NaN
if $\nu = 0$ **then**
 $\quad \lfloor$ **if** $\mathbf{x}' = 0$ **then**
 $\quad \quad \lfloor$ **return** $-\exp(-2\pi i \mathbf{x} \cdot \mathbf{y}')$
 $\quad \quad \lfloor$ **return** 0
if $\nu \in -2\mathbb{N}_+$ **then**
 $\quad \lfloor$ **return** 0
4. **Kahan summation in real and reciprocal space**
sum_real = 0 sum_reciprocal = 0
if $\text{regularised} = \text{False}$ **then**
 $\quad \lfloor$ **for** $\mathbf{z} \in A\mathbb{Z}^d : |\mathbf{z} - \mathbf{x}'| \leq r$ **do**
 $\quad \quad \lfloor$ sum_real += $G_\nu(\mathbf{z} - \mathbf{x}') \exp(-2\pi i \mathbf{z} \cdot \mathbf{y}')$
 $\quad \quad \lfloor$ **for** $\mathbf{k} \in A^{-T}\mathbb{Z}^d : |\mathbf{k} + \mathbf{y}'| \leq r$ **do**
 $\quad \quad \quad \lfloor$ sum_reciprocal += $G_{d-\nu}(\mathbf{k} + \mathbf{y}') \exp(2\pi i \mathbf{x}' \cdot (\mathbf{k} + \mathbf{y}'))$
 $\quad \quad \quad \lfloor$ sum_real *= $\exp(-2\pi i \mathbf{y}' \cdot (\mathbf{x} - \mathbf{x}'))$
 $\quad \quad \quad \lfloor$ sum_reciprocal *= $\exp(-2\pi i \mathbf{y}' \cdot (\mathbf{x} - \mathbf{x}'))$
else if $\text{regularised} = \text{True}$ **then**
 $\quad \lfloor$ **for** $\mathbf{z} \in A\mathbb{Z}^d : |\mathbf{z} - \mathbf{x}'| \leq r$ **do**
 $\quad \quad \lfloor$ sum_real += $G_\nu(\mathbf{z} - \mathbf{x}') \exp(-2\pi i (\mathbf{z} \cdot \mathbf{y}' - \mathbf{y}' \cdot \mathbf{x}'))$
 $\quad \quad \lfloor$ **for** $\mathbf{k} \in (A^{-T}\mathbb{Z}^d) \setminus \{\mathbf{y}'\} : |\mathbf{k} + \mathbf{y}'| \leq r$ **do**
 $\quad \quad \quad \lfloor$ sum_reciprocal += $G_{d-\nu}(\mathbf{k} + \mathbf{y}') \exp(2\pi i \mathbf{x}' \cdot (\mathbf{k} - (\mathbf{y}' - \mathbf{y}')))$
 $\quad \quad \quad \lfloor$ sum_reciprocal += $G_{d-\nu, \lambda}^{\text{reg}}(\mathbf{y}')$
5. **Postprocessing**
return $a^{-\nu} \pi^{\nu/2} (\text{sum_real} + \text{sum_fourier}) / \Gamma(\nu/2)$

Proof. Since the range of $\lfloor \cdot \rfloor$ is \mathbb{Z}^d , $\mathbf{v}_x \in \Lambda$. The statement follows by applying

$$-\frac{1}{2} \leq w - \lfloor w + 1/2 \rfloor < \frac{1}{2}, \quad w \in \mathbb{R}$$

in every component of

$$A^{-1}(\mathbf{x} - \mathbf{v}) = A^{-1}\mathbf{x} - \lfloor A^{-1}\mathbf{x} + \mathbf{1}/2 \rfloor. \quad \square$$

3.2. Special cases. For specific values of ν , poles are encountered in the gamma function or in the Crandall functions. These special cases need to be treated separately in order to guarantee a stable evaluation.

In Algorithm 1, when $\mathbf{y} \in \Lambda^*$, the pole of the Epstein zeta function at $\nu = d$ is indicating directly without evaluating the Crandall representation. At the removable singularities $\nu \in -2\mathbb{N}_0$ of the gamma function, we return the appropriate limiting value, as shown in the following lemma.

Lemma 3.2. *Let Λ be a d -dimensional lattice, $\mathbf{x}, \mathbf{y} \in \mathbb{R}^d$ and $k \in \mathbb{N}_0$. Then*

$$Z_{\Lambda, -2k} \begin{vmatrix} \mathbf{x} \\ \mathbf{y} \end{vmatrix} = \begin{cases} -e^{-2\pi i \mathbf{x} \cdot \mathbf{y}} & k = 0 \text{ and } \mathbf{x} \in \Lambda \\ 0 & \text{otherwise} \end{cases}.$$

Proof. Let $\nu \in \mathbb{C} \setminus (-2\mathbb{N}_0)$ and $\mathbf{x} \notin \Lambda$, then

$$G_\nu(\mathbf{z} - \mathbf{x})e^{-2\pi i \mathbf{y} \cdot \mathbf{z}}, \quad \mathbf{z} \in \Lambda$$

and

$$G_{d-\nu}(\mathbf{k} + \mathbf{y})e^{-2\pi i \mathbf{x} \cdot (\mathbf{k} + \mathbf{y})}, \quad \mathbf{k} \in \Lambda^*$$

are bounded for $\nu \rightarrow -2k$ due to Lemma 2.9, and

$$G_{d-\nu}(\mathbf{0})e^{-2\pi i \mathbf{x} \cdot \mathbf{0}} = \frac{1}{d - \nu}.$$

Since $1/\Gamma(\nu/2) \rightarrow 0$ for $\nu \rightarrow -2k$, Crandall's representation implies that the Epstein zeta function evaluates to zero for $\nu \in -2\mathbb{N}_0$. Now let $\mathbf{x} \in \Lambda$, so there is an additional summand of the form

$$G_\nu(\mathbf{0})e^{-2\pi i \mathbf{y} \cdot \mathbf{x}} = -\frac{2}{\nu}e^{-2\pi i \mathbf{y} \cdot \mathbf{x}}$$

in Crandall's representation. The Epstein zeta still evaluates to zero for $\nu \rightarrow -2\mathbb{N}_+$ and

$$-\frac{\pi^{\nu/2}}{\Gamma(\nu/2)} \frac{2}{\nu} e^{-2\pi i \mathbf{y} \cdot \mathbf{x}} = -\frac{\pi^{\nu/2}}{\Gamma(\nu/2 + 1)} e^{-2\pi i \mathbf{y} \cdot \mathbf{x}} \rightarrow -e^{-2\pi i \mathbf{y} \cdot \mathbf{x}}, \quad \nu \rightarrow 0. \quad \square$$

3.3. Truncation and compensated summation. In this subsection, we present a rigorous error bound when truncating the sums in Crandall's representation. The proof is provided in Appendix C.

Theorem 3.3 (Remainder estimate). *Let $\Lambda = AZ^{d \times d}$, for $A \in \mathbb{R}^{d \times d}$ regular and $\det(A) = 1$. Let $\mathbf{x}, \mathbf{y} \in \mathbb{R}^d$ and let $\nu \in I$ with $I \subset \mathbb{R}$ compact so that $\nu \neq d$ if $\mathbf{y} \in \Lambda^*$. Let R denote the remainder obtained by truncation at $r > 0$ in Crandall's representation*

$$Z_{\Lambda, \nu} \begin{vmatrix} \mathbf{x} \\ \mathbf{y} \end{vmatrix} = \frac{\pi^{\nu/2}}{\Gamma(\nu/2)} \left[\sum_{\substack{\mathbf{z} \in \Lambda \\ |\mathbf{z} - \mathbf{x}| \leq r}} G_\nu(\mathbf{z} - \mathbf{x})e^{-2\pi i \mathbf{y} \cdot \mathbf{z}} + \frac{1}{V_\Lambda} \sum_{\substack{\mathbf{k} \in \Lambda^* \\ |\mathbf{k} + \mathbf{y}| \leq r}} G_{d-\nu}(\mathbf{k} + \mathbf{y})e^{2\pi i \mathbf{x} \cdot (\mathbf{k} + \mathbf{y})} \right] + \mathcal{R}_\Lambda(r).$$

d	1	2	3	4	5	6	7	8	9	10
r_0	3.8	3.9	4.	4.1	4.2	4.2	4.3	4.4	4.4	4.5

TABLE 1. Truncation values r_0 to achieve a truncation error $\mathcal{R}_{\mathbb{Z}^d} < 10^{-18}$ in Crandall's representation for and $-10 \leq \nu \leq 10$ obtained by Theorem 3.3 for the choice of $\varepsilon = 1/20$.

Then, for any $\varepsilon > 0$ and $r > (1 + 2\varepsilon)\sqrt{d}\kappa(A)$ with the condition number $\kappa(A) = \|A\|\|A^{-1}\|$, where $\|\cdot\|$ denotes the spectral norm, it holds that

$$|\mathcal{R}_\Lambda(r)| < \kappa(A)^{d+1} \sup_{\nu \in I} c_\nu \left(R_\nu(r/\kappa(A)) + R_{d-\nu}(r/\kappa(A)) \right)$$

with the prefactor

$$c_\nu = \frac{(3/2)^{d\pi(\nu+d)/2}}{\Gamma(d/2 + 1)|\Gamma(\nu/2)|}$$

and with the function

$$R_\nu(r) = \frac{r^{d+1}}{\varepsilon} \left(\frac{G_{d+1}(r-\varepsilon) - G_\nu(r-\varepsilon)}{d+1-\nu} \right),$$

where the limit $\nu \rightarrow d+1$ is well-defined. In particular,

$$\mathcal{R}_\Lambda(\kappa(A)r) \leq \kappa(A)^{d+1} \mathcal{R}_{\mathbb{Z}^d}(r).$$

For practical purposes, a sufficient upper bound to the error in Theorem 3.3 is obtained by choosing $\varepsilon = 1/20$. We present sufficient truncation values $r = r_0$ for achieving machine precision for the square lattice $\Lambda = \mathbb{Z}^d$ as a function of dimension d in Table 1. The corresponding value for general lattices $\Lambda = A\mathbb{Z}^d$ where $\det(A) = 1$ is then obtained as

$$r = \kappa(A)r_0,$$

where the error lies below machine precision if $\kappa(A)^{d+1} \leq 10^2$ for the values r_0 in Table 1.

In infinite precision arithmetic, a truncation value based on Theorem 3.3 guarantees that the the desired precision is reached when computing the Epstein zeta function. However, in floating point arithmetic, roundoff errors accumulate in the evaluation of the sums for large dimensions d , which can exceed the rigorous truncation error bound by several orders of magnitude. A practical solution that significantly reduces the roundoff error is provided by the compensated summation algorithm developed by Kahan [32]. Here, a separate compensator variable is introduced, which stores an estimation for the accumulated error. Using compensated summation, we show in Section 5 that our resulting algorithm reaches machine precision across all test cases even for large dimensions d . An alternative, albeit more computationally expensive, approach involves dividing the summation ball into shells and performing the summation in reverse order, starting from the outermost shell with the smallest absolute values and progressing toward the inner shells.

3.4. Evaluation of the incomplete gamma functions. A stable, fast, and accurate evaluation of the incomplete gamma function is the foundation of any algorithm relying on Crandall's representation of the Epstein zeta function. A wide range of algorithms focuses on evaluating $\Gamma(\nu, x)$ at the restricted parameter

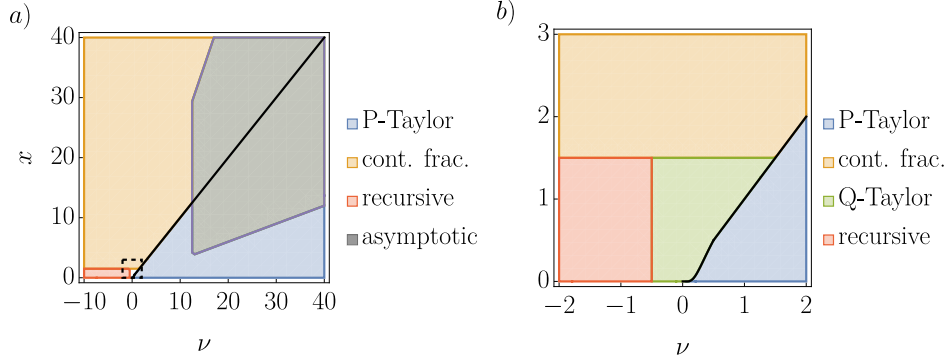


FIGURE 2. Regions of different evaluation methods of the incomplete Gamma functions (a). Panel (b) offers a magnified view of the region close to the origin.

range $\nu > 0$, see for example Ref [1, 26]. Implementations in arbitrary precision libraries such as Arb and FLINT [31] guarantee correct results but are not usable in high-performance applications due to long evaluation times. Fast and stable implementations based on the work of [25] only offer single precision. Therefore no existing implementation is sufficient for a reliable high-performance implementation of the Epstein zeta function. We address this problem and provide a fast and precise implementation based on the work of [25, 26] that evaluates the incomplete Gamma function to full precision over the whole parameter range. In the following, we discuss the underlying methods.

The algorithm is based on evaluating the regularisation of the incomplete Gamma functions in the first parameter.

Definition 3.4. Let $x, \nu > 0$. Then, we define the incomplete gamma function ratios

$$P(\nu, x) = \frac{\gamma(\nu, x)}{\Gamma(\nu)}, \quad Q(\nu, x) = \frac{\Gamma(\nu, x)}{\Gamma(\nu)}.$$

Depending on the values of x and ν , different methods for computing these functions need to be applied. The regions corresponding to the different evaluation methods as functions of x and ν are illustrated in Figure 2.

By construction, the range of both P and Q equals $[0, 1]$ and we have $P + Q = 1$. We aim to compute P whenever $Q > P$, and Q if $Q < P$. The black line in Figure 2 indicates an approximation of this separation, where we compute P whenever

$$x < \begin{cases} 2^{1-1/\nu} & 0 < \nu < \frac{1}{2} \\ \nu & \nu \geq \frac{1}{2} \end{cases}$$

and compute Q otherwise.

The computation of P (blue region) is performed via the power series

$$P(\nu, x) = \frac{x^\nu e^{-x}}{\Gamma(\nu + 1)} \sum_{n=0}^{\infty} \frac{x^n}{(\nu + 1)_n},$$

which can be derived through integration by parts. Here,

$$(\nu + 1)_n = \Gamma(\nu + n + 1)/\Gamma(\nu + 1)$$

denotes the rising Pochhammer symbol. The above Taylor series converges for $\nu > -1$ and arbitrary x .

From this power series, we can derive a power series for Q (green region). We write $Q = 1 - P = u + v$, where

$$u = 1 - \frac{1}{\Gamma(\nu + 1)} + \frac{1 - x^\nu}{\Gamma(\nu + 1)}$$

and

$$v = \frac{x^\nu}{\Gamma(\nu + 1)}(1 - \Gamma(\nu + 1)x^{-\nu}P(\nu, x)).$$

The term v can be evaluated using the power series above. For the term u , we evaluate the parts

$$1 - \frac{1}{\Gamma(\nu + 1)}$$

and

$$\frac{1 - x^\nu}{\Gamma(\nu + 1)}$$

separately using their Taylor series expansions. Details can be found in [25]. This method works for arbitrary x and $\nu > -1$, and the relative error grows with x . We apply this method of computing Q for $\nu > -1/2$ and $x < x_0 = 3/2$.

Another method to compute Q is given by the continued fraction expansion (orange region),

$$x^{-\nu} e^x \Gamma(\nu, x) = \frac{1}{x + \frac{1 - \nu}{1 + \frac{1}{x + \frac{2 - \nu}{1 + \frac{2}{x + \frac{3 - \nu}{1 + \frac{3}{x + \dots}}}}}}}$$

attributed to Legendre. A proof can be found in [48]. Details for evaluating the continued fraction can be found in [25]. This continued fraction corresponds to an asymptotic expansion at $x \rightarrow \infty$ and thus, it converges fast for large x . However, the convergence deteriorates for $x \approx \nu$.

For large x and large ν , we use the uniform asymptotic expansion (grey region) derived in [45]. Details on the computation can be found in [26] and [44].

For negative ν and $x < x_0$, we use a recurrence relation (red region). Here, we make use of the regularisation

$$G(\nu, x) = e^x x^{-\nu} \Gamma(\nu, x).$$

Integration by parts gives the recurrence relation

$$G(-n + \varepsilon, x) = \frac{1}{n - \varepsilon}(1 - xG(-n + 1 + \varepsilon, x)),$$

where we assume $-1/2 \leq \varepsilon \leq 1/2$ and $n \in \mathbb{N}_+$. $G(\varepsilon, x)$ can be evaluated using the methods described above. A stability discussion of this recursion pattern can be found in [25]; for $x_0 = 3/2$, the relative error of $G(\varepsilon, x)$ is amplified by at most 5.7.

To compute the lower incomplete gamma function, we can use the previous considerations to get a modified algorithm. Instead of using the series expansion for the functions P and Q , we directly evaluate γ^* with a similar series. For negative ν , specialized evaluation is required at $\nu \in -\mathbb{N}_+$ and at $x = 0$. It turns out to be advantageous to avoid the recurrence relation around $\nu = -1/2$ for small x . Here, we also use the series expansion for γ^* .

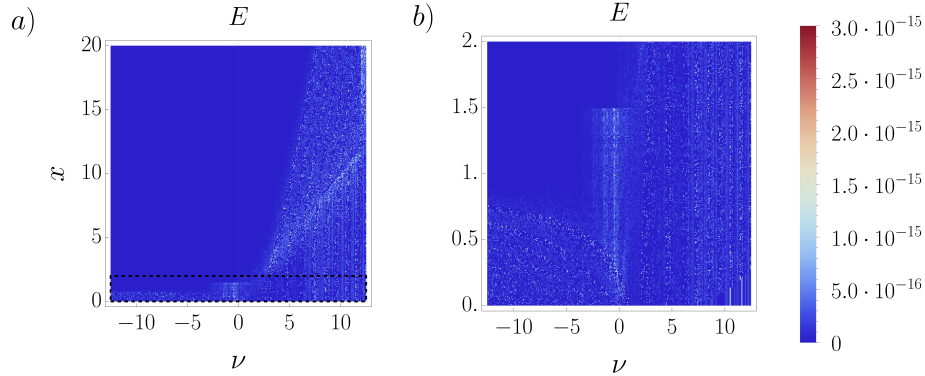


FIGURE 3. Minimum of absolute and relative error of our implementation of the upper incomplete gamma function compared to the arbitrary precision result from [30]. The dashed black box in (a) outlines the magnified region shown in (b).

4. EPSTEINLIB

We have created an open-source, high-performance library in C, called EpsteinLib, which implements the algorithm for the Epstein zeta function as well as its regularisation for any dimension, any lattice, any real exponent ν and $\mathbf{x}, \mathbf{y} \in \mathbb{R}^d$. It is available on github.com/epsteinlib and includes a Python wrapper. The Epstein zeta function is implemented in this library as

```

1 double complex epsteinZeta(
2     double nu,
3     unsigned int dim,
4     const double *A,
5     const double *x,
6     const double *y);

```

and the regularised Epstein zeta function as

```

1 double complex epsteinZetaReg(
2     double nu,
3     unsigned int dim,
4     const double *A,
5     const double *x,
6     const double *y);

```

which evaluates to full precision over the whole parameter range up to ten dimensions. For instance, it allows for the precise and efficient computation of Madelung constants of arbitrary materials. Here, we provide an example for NaCl (see [11] for a reference value)

```

1  #include <complex.h>
2  #include <math.h>
3  #include <stdio.h>
4  #include "epsteinZeta.h"
5
6  int main() {
7
8      // Madelung constant found in literature
9      double madelungRef = -1.7475645946331821906362120355443974;
10     unsigned int dim = 3;
11     double m[] = {1, 0, 0, 0, 1,
12                  0, 0, 0, 1}; // identity matrix for whole numbers
13     double x[] = {0, 0, 0}; // no shift
14     double y[] = {0.5, 0.5, 0.5}; // alternating sum
15     double nu = 1.0;
16     double madelung = creal(epsteinZeta(nu, dim, m, x, y));
17     printf("Madelung sum in 3 dimensions:\t %.16lf\n", creal(madelung));
18     printf("Reference value:\t\t %.16lf\n", madelungRef);
19     printf("Relative error:\t\t\t +%.2e\n",
20           fabs(madelungRef - madelung) / fabs(madelungRef));
21
22     return fabs(madelung - madelungRef) > pow(10, -14);
23 }

```

In addition to the C library, we provide a Python wrapper for accessibility, which can be installed with

```
1 pip install epsteinlib
```

as well as a Mathematica wrapper. In the Python package, the Epstein zeta function is implemented as

```

1  def epstein_zeta(
2      nu: float | int,
3      A: NDArray[np.float64],
4      x: NDArray[np.float64],
5      y: NDArray[np.float64]) -> complex:

```

and the regularised Epstein zeta function as

```

1  def epstein_zeta_reg(
2      nu: float | int,

```

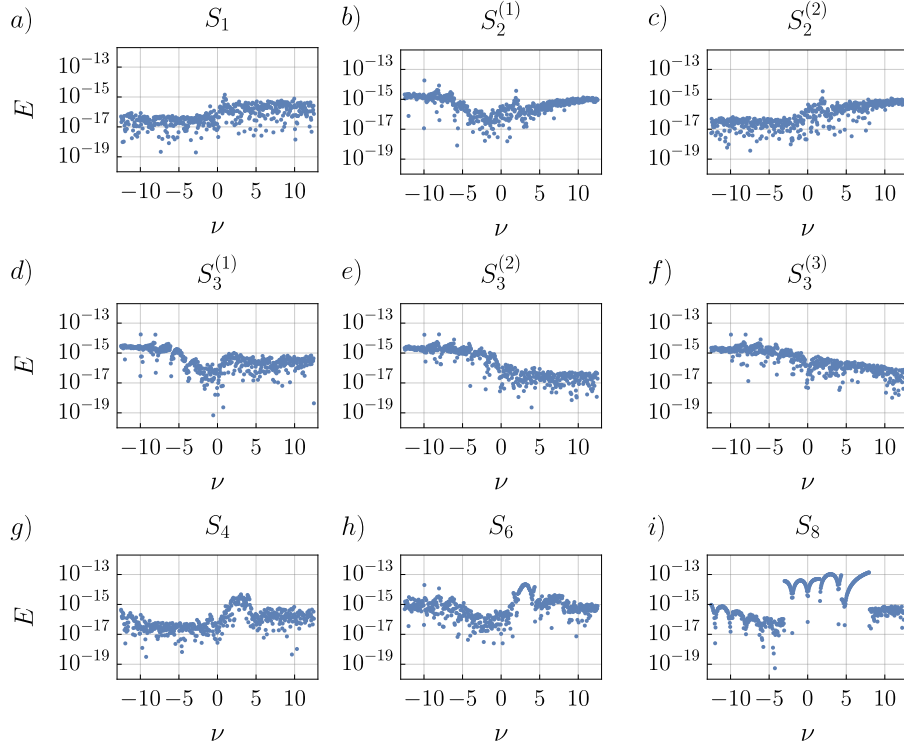


FIGURE 4. Minimum of absolute and relative error of the Epstein zeta function for the values as in Table 2. The errors of the regularised function are approximately equal, see Table 3.

```

3   A: ndarray[np.float64],
4   x: ndarray[np.float64],
5   y: ndarray[np.float64]) -> complex:

```

5. NUMERICAL EXPERIMENTS

This section provides a detailed analysis of the error and runtime of our algorithm for an extensive set of parameters. To benchmark the error of our algorithm, known formulas for special cases of the lattice sums

$$S_d = Z_{\Lambda, \nu} \begin{vmatrix} \mathbf{x} \\ \mathbf{y} \end{vmatrix}$$

from Refs. [16, 55, 12] in $d = 1, 2, 3, 4, 6, 8$ dimensions are collected. The particular choices for \mathbf{x} , \mathbf{y} , and A as well the resulting analytical formulas for elementary function are provided in Table 2. Here η denotes the Dirichlet eta function

$$\eta(\nu) = (1 - 2^{1-\nu})\zeta(\nu),$$

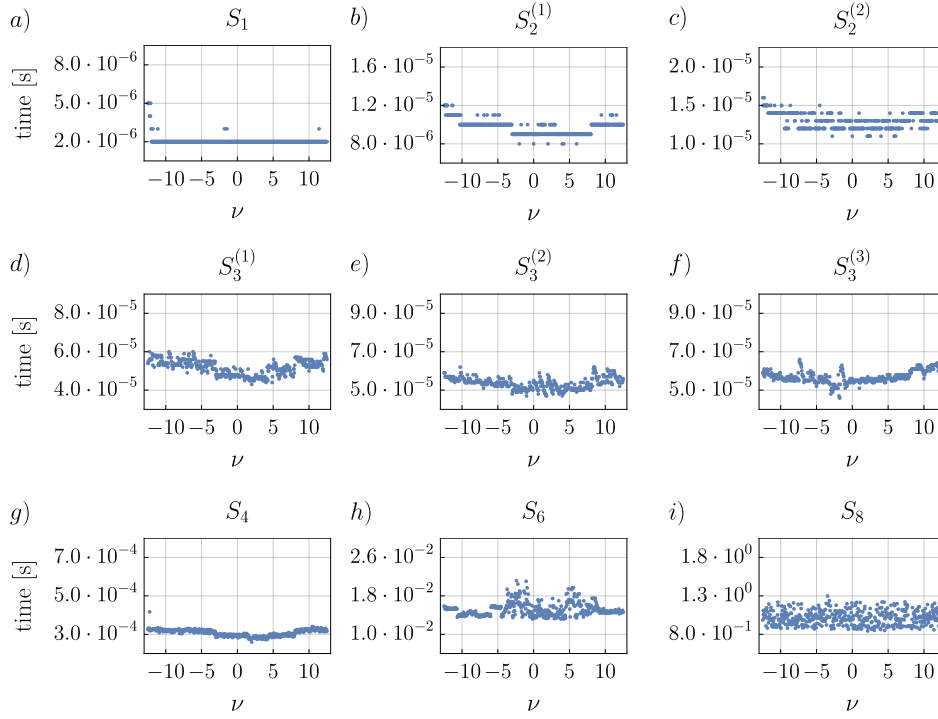


FIGURE 5. Evaluation times of the Epstein zeta function of the Epstein zeta function for the values as in Table 2. The evaluation times of the regularised function are approximately equal, see Table 3.

λ the Dirichlet lambda function,

$$\lambda(\nu) = (1 - 2^{-\nu})\zeta(\nu)$$

and β the Dirichlet beta function,

$$\beta(\nu) = 4^{-\nu}(\zeta(\nu, 1/4) - \zeta(\nu, 3/4)).$$

The function $\zeta(\cdot)$ with one complex argument is the Riemann zeta function and for any $x > 0$, the function $\zeta(\cdot, x)$ denotes the Hurwitz zeta function, given by the meromorphic continuation of

$$\zeta(\nu, x) = \sum_{n=0}^{\infty} \frac{1}{(n+x)^{\nu}}, \quad \operatorname{Re}(\nu) > 1$$

to $\nu \in \mathbb{C}$, see Ref. [17, Section §25.11(i)]. Note that the regularised Epstein zeta function follows from Def. 2.14 and agrees with the Epstein zeta function in the case $\mathbf{y} = 0$ if $\nu \neq d$. We evaluate the analytical formulas for $\nu = -12.5 + \varepsilon, \dots, 12.5 + \varepsilon$ for $\varepsilon = 2^{-15}$ in increments of 0.05 in Mathematica with 200 digits and measure the minimum of relative and absolute error

$$E = \min(E_{\text{abs}}, E_{\text{rel}})$$

Sum	d	A	\mathbf{x}	\mathbf{y}	value
S_1	1	$\mathbf{1}$	$-\mathbf{e}^{(1)}/2$	$\mathbf{0}$	$2\zeta(\nu, 1/2)$
$S_2^{(1)}$	2	$\text{diag}(1, 2)$	$-\mathbf{e}^{(1)} - 2\mathbf{e}^{(2)}$	$\mathbf{0}$	$2(1 - 2^{-\nu/2} + 2^{1-\nu})$ $\times \zeta(\nu/2)\beta(\nu/2)$
$S_2^{(2)}$	2	$\begin{pmatrix} 1 & 1/2 \\ 0 & \sqrt{3}/2 \end{pmatrix}$	$\mathbf{0}$	$\mathbf{0}$	$3^{1-\nu/2}2\zeta(\nu/2)$ $\times (\zeta(\nu/2, 1/3) - \zeta(\nu/2, 2/3))$
$S_3^{(1)}$	3	$\text{diag}(1, 1, 2)$	$-\mathbf{e}^{(3)}/2$	$\mathbf{e}^{(1)}/2$	$4^{\nu/2}\beta(\nu - 1)$
$S_3^{(2)}$	3	$\text{diag}(6, 6, 6)$	$-\mathbf{1}$	$\mathbf{1}/12$	$3^{-\nu/2}\beta(\nu - 1)$
$S_3^{(3)}$	3	$\text{diag}(2\sqrt{2}, 4, 2)$	$-\mathbf{e}^{(2)} - \mathbf{e}^{(3)}$	$\mathbf{e}^{(1)}/(4\sqrt{2})$	$2^{1-\nu/2}\beta(\nu - 1)$
S_4	4	$\mathbf{1}$	$\mathbf{e}^{(1)}/2$	$\mathbf{0}$	$2^\nu(\beta(\nu/2)\beta(\nu/2 - 1)$ $+ \lambda(\nu/2)\lambda(\nu/2 - 1))$
S_6	6	$\mathbf{1}$	$\mathbf{0}$	$(\mathbf{e}^{(1)} + \mathbf{e}^{(2)})/2$	$4\beta(\nu/2 - 2)\eta(\nu/2)$
S_8	8	$\mathbf{1}$	$\mathbf{0}$	$\mathbf{1}/2$	$-16\eta(\nu/2 - 3)\zeta(\nu/2)$

TABLE 2. Analytic formulas for special cases of the Epstein zeta function for $\Lambda = \mathbb{Z}^{d \times d}$ in $d = 1, 2, 4, 6, 8$ dimensions. Here, $\mathbf{1} \in \mathbb{R}^{d \times d}$ is the unit matrix, $\text{diag}(a_1, \dots, a_d) \in \mathbb{R}^{d \times d}$ is the diagonal matrix with diagonal entries a_1, \dots, a_d , the unit vector $\mathbf{e}^{(i)} \in \mathbb{R}^d$ has the components $e_j^{(i)} = \delta_{ij}$ for $1 \leq i, j \leq d$ and the one-vector is defined as $\mathbf{1} = (1, \dots, 1)^T \in \mathbb{R}^d$.

of our implementation both for the normal and the regularised Epstein zeta function. The offset ε is chosen, to avoid instant evaluation in the special cases of our algorithm, which would distort the timing benchmarks. The runtime and precision of our algorithm for both the standard and regularised Epstein zeta function are summarized in Table 3.

We display the error as a function of ν in Figure 4. We obtain full precision over the complete ν -range, with the maximum error rising mildly from 1.6×10^{-15} for $d = 1$ to 10^{-13} for large dimension $d = 8$. The small increase in the error of the regularised Epstein zeta function around $\nu = d + 2\mathbb{N}_0$ is unavoidable and results from the singularities of the Fourier transform of $|\cdot|^{-\nu}$.

In Figure 5, we display the runtime of our algorithm for computing the sums S_d as a function of ν . The values were obtained on an Intel Core i7-1260P (12th Gen) 16-core processor with 32 GB of RAM. Here, the runtime only mildly depends on the choice of ν , as well as of \mathbf{x} and \mathbf{y} . Our implementation allows for the computation of 2D sums in less than 20 microseconds and 4D sums in less than 0.3 milliseconds. Even 8D sums become accessible with a runtime of less than 2 seconds on a standard laptop.

6. PHYSICAL APPLICATIONS

The Epstein zeta function forms the basis for studying long-range interacting classical and quantum systems with applications ranging from the computation of Madelung constants in theoretical chemistry [40, 11], over unconventional superconductivity [10], to high energy physics [49, 3]. In this section, we use our

sum	type	E_{\max}	$t_{\min} - t_{\max} [s]$	$t_{\text{avg}} [s]$
S_1	non-reg	$1.4 \cdot 10^{-15}$	$2 \cdot 10^{-6} - 5 \cdot 10^{-6}$	$2.1 \cdot 10^{-6}$
	reg	$1.6 \cdot 10^{-15}$	$2 \cdot 10^{-6} - 6 \cdot 10^{-6}$	$2.1 \cdot 10^{-6}$
$S_2^{(1)}$	non-reg	$1.8 \cdot 10^{-14}$	$8 \cdot 10^{-6} - 1.2 \cdot 10^{-5}$	$9.7 \cdot 10^{-6}$
	reg	$1.8 \cdot 10^{-14}$	$9 \cdot 10^{-6} - 1.3 \cdot 10^{-5}$	$1.0 \cdot 10^{-5}$
$S_2^{(2)}$	non-reg	$3.4 \cdot 10^{-15}$	$1.1 \cdot 10^{-5} - 1.6 \cdot 10^{-5}$	$1.3 \cdot 10^{-5}$
	reg	$3.4 \cdot 10^{-15}$	$1.1 \cdot 10^{-5} - 1.6 \cdot 10^{-5}$	$1.3 \cdot 10^{-5}$
$S_3^{(1)}$	non-reg	$1.8 \cdot 10^{-14}$	$4.3 \cdot 10^{-5} - 6 \cdot 10^{-5}$	$5.2 \cdot 10^{-5}$
	reg	$1.8 \cdot 10^{-14}$	$4.3 \cdot 10^{-5} - 6.1 \cdot 10^{-5}$	$5.2 \cdot 10^{-5}$
$S_3^{(2)}$	non-reg	$1.8 \cdot 10^{-14}$	$4.7 \cdot 10^{-5} - 6.2 \cdot 10^{-5}$	$5.3 \cdot 10^{-5}$
	reg	$1.8 \cdot 10^{-14}$	$4.7 \cdot 10^{-5} - 6.2 \cdot 10^{-5}$	$5.3 \cdot 10^{-5}$
$S_3^{(3)}$	non-reg	$1.7 \cdot 10^{-14}$	$4.6 \cdot 10^{-5} - 6.6 \cdot 10^{-5}$	$5.7 \cdot 10^{-5}$
	reg	$1.7 \cdot 10^{-14}$	$4.5 \cdot 10^{-5} - 6.5 \cdot 10^{-5}$	$5.7 \cdot 10^{-5}$
S_4	non-reg	$4.7 \cdot 10^{-15}$	$2.6 \cdot 10^{-4} - 4.2 \cdot 10^{-4}$	$3.1 \cdot 10^{-4}$
	reg	$4.7 \cdot 10^{-15}$	$2.7 \cdot 10^{-4} - 3.4 \cdot 10^{-4}$	$3.1 \cdot 10^{-4}$
S_6	non-reg	$2.3 \cdot 10^{-14}$	$1.3 \cdot 10^{-2} - 2.1 \cdot 10^{-2}$	$1.5 \cdot 10^{-2}$
	reg	$2.1 \cdot 10^{-14}$	$1.3 \cdot 10^{-2} - 2.1 \cdot 10^{-2}$	$1.5 \cdot 10^{-2}$
S_8	non-reg	$1.4 \cdot 10^{-13}$	$8.4 \cdot 10^{-1} - 1.3 \cdot 10^0$	$1.0 \cdot 10^0$
	reg	$1.0 \cdot 10^{-13}$	$8.5 \cdot 10^{-1} - 1.3 \cdot 10^0$	$1.0 \cdot 10^0$

TABLE 3. Performance and accuracy of the algorithm, compared to analytic representations as in Table 2. The lower index d of the sum $S_d^{(j)}$ indicates the lattice dimension.

efficiently implemented Epstein zeta function to explore two relevant systems arising in condensed matter and quantum physics.

6.1. Anomalous quantum spin-wave dispersion in 3D. In our first application, we study linear spin waves in a quantum spins lattice Λ with power-law long-range interactions. The properties of the system are then determined by the Hamiltonian

$$H = -\frac{J}{2} \sum'_{\mathbf{x}, \mathbf{y} \in \Lambda} \frac{\mathbf{S}_{\mathbf{x}} \cdot \mathbf{S}_{\mathbf{y}}}{|\mathbf{x} - \mathbf{y}|^\nu},$$

where $\mathbf{S}_{\mathbf{x}}$ is the spin operator at lattice site \mathbf{x} and $J > 0$ determines the ferromagnetic interaction between nearest neighbors. Following standard techniques (Holstein-Primakoff transformation and limit of large spin quantum numbers $S \gg 1$), a plane wave Ansatz yields the dispersion relation, that relates the temporal frequency $\omega(\mathbf{k})$ of a plane wave in the system to its spatial period determined through the wavevector \mathbf{k} . For general lattices Λ and interaction exponents ν , this dispersion relation takes the form [10, Appendix D]

$$\hbar\omega(\mathbf{k}) = JS \left(Z_{\Lambda, \nu} \begin{vmatrix} \mathbf{0} \\ \mathbf{0} \end{vmatrix} - Z_{\Lambda, \nu} \begin{vmatrix} \mathbf{0} \\ \mathbf{k} \end{vmatrix} \right),$$

with \hbar the reduced Planck constant.

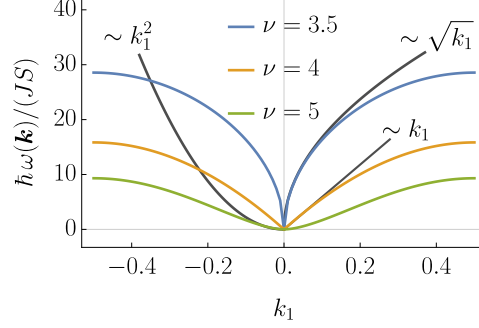


FIGURE 6. Quantum spin wave dispersion relation of spins on a 3D square lattice $\Lambda = \mathbb{Z}^3$ as a function of k_1 for $k_2 = k_3 = 0$. Typical scaling $\omega(\mathbf{k}) \sim \mathbf{k}^2$ is observed for $\nu \geq d + 2$ (green line $\nu = 5$), whereas anomalous scaling is observed for $d < \nu < d + 2$ (orange line $\nu = 4$, blue line $\nu = 3 + 1/2$).

In Figure 6, we display the dispersion relation for a 3D square lattice $\Lambda = \mathbb{Z}^3$ as a function of k_1 along the cut $k_2 = k_3 = 0$ for different values of the interaction exponent ν . Of central interest is here the behavior at small wavevectors, corresponding to the low-energy sector. While for $\nu = 5$ (green), the dispersion relation follows the well-known \mathbf{k}^2 behavior of short-range interacting systems, anomalous behavior is observed for $\nu < d + 2$. In the case of $\nu = d + 1$ (orange line), a linear dispersion relation is obtained, which is the three-dimensional equivalent of the result obtained in [36] for dipole-dipole interactions $1/|\mathbf{r}|^3$ in two dimensions and generalizes the result in one dimension from Ref. [51]. For $\nu = 3.5$ (blue), a square root behavior around $\mathbf{k} = \mathbf{0}$ is observed.

This result can be understood from the regularised Epstein zeta function in Definition 2.14, which yields for the small $|\mathbf{k}|$ behavior

$$\hbar\omega(\mathbf{k}) = JS(c_\nu |\mathbf{k}|^{\nu-d} + \mathcal{O}(\mathbf{k}^2)),$$

with a constant $c_\nu \in \mathbb{R}$. Hence for $d < \nu < d + 2$, the singularity of Epstein zeta dominates the low energy behavior, leading to an anomalous scaling $\omega(\mathbf{k}) \sim |\mathbf{k}|^{\nu-d}$. For $\nu = d$, the dispersion relation becomes unbounded from below as

$$Z_{\Lambda,\nu} \Big|_{\mathbf{k}}^{\mathbf{0}} \sim \log(|\mathbf{k}|^2)$$

signaling a breakdown of the model, which is often associated with a phase transition.

Our work offers to study long-range dispersion relations both numerically, by using our algorithm implemented in EpsteinLib, as well as on an analytical basis using our analysis of the properties of the Epstein zeta function and its regularisation for any lattice and any interaction exponent.

6.2. Casimir effect. The Casimir effect states that an attractive force acts between two perfectly conducting plates due to quantum fluctuations of the electromagnetic field. Originally derived by Casimir and Polder in 1948, it can be interpreted either as a result of retarded Van-der-Waals forces [13] or due to pressure associated with the spontaneous creation and annihilation of photons in vacuum [14]. The resulting forces can dominate the physics at microscopic scales, are measurable

in state-of-the-art experiments [38], and recently have been demonstrated to be tunable from attractive to repulsive in ferrofluids [53], with various technological applications such as quantum levitation [54]. Our implementation of the Epstein zeta function in EpsteinLib allows for numerical investigation of the Casimir energy for a wide range of geometries Λ in any dimension; we present two examples.

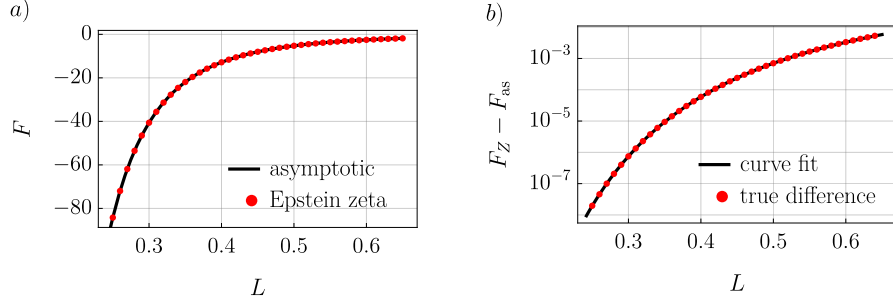


FIGURE 7. Comparison of the asymptotic expression of the force $F = F_{\text{as}}$ of the Casimir effect and the force as the discrete derivative of the Epstein zeta function $F = F_Z$ as a function of the small edge L (a). The difference between the asymptotic and the Epstein zeta function is small only for small edges, and the true force is bigger than the asymptotic expression for long edges (b).

Consider the d -dimensional hypercuboidal region E_Λ described by the lattice matrix $A = \text{diag}(L_1, \dots, L_d)$ captures the information of the geometry of the edge-lengths $0 < L_1, \dots, L_d < \infty$. The Klein-Gordon wave equation for a non-interacting scalar field with mass $m \geq 0$, natural units $c = \hbar = 1$ and periodic boundary conditions reads

$$\begin{aligned} (\partial_t^2 - \Delta + m^2)\phi(t, \mathbf{x}) &= 0, & t \in \mathbb{R}, \mathbf{x} \in E_\Lambda \\ \phi(t, \mathbf{x}) &= \phi(t, \mathbf{x} + \mathbf{L}_\mathbf{x}), & t \in \mathbb{R}, \mathbf{x} \in \partial E_\Lambda \end{aligned}$$

where $(\mathbf{L}_\mathbf{x})_i = -L_i \text{sign } x_i$ for $1 \leq i \leq d$. A solution is given in terms of the field modes

$$\phi(t, \mathbf{x}) = e^{-i\lambda_{\mathbf{k}}t} e^{i\mathbf{k} \cdot \mathbf{x}}$$

with eigenvalues

$$\lambda_{\mathbf{k}} = \sqrt{m^2 + \mathbf{k}^2}$$

where $\mathbf{k} = 2\pi(z_1/L_1, \dots, z_d/L_d)^T$ for $\mathbf{z} \in \mathbb{Z}^d$. The total energy \mathcal{E} is given by

$$\mathcal{E}(\Lambda) = \frac{1}{2} \sum_{\mathbf{k}} \lambda_{\mathbf{k}}^{-\nu} \Big|_{\nu=-1}$$

in the sense of evaluating the meromorphic continuation in $\nu \in \mathbb{C}$ of the lattice sum at $\nu = -1$, see Ref. [35, 19, 3]. In the massless case $m = 0$ we obtain a representation in terms of the Epstein zeta function as

$$\mathcal{E}(\Lambda) = \pi Z_{\Lambda^*, -1} \Big|_{\mathbf{0}}$$

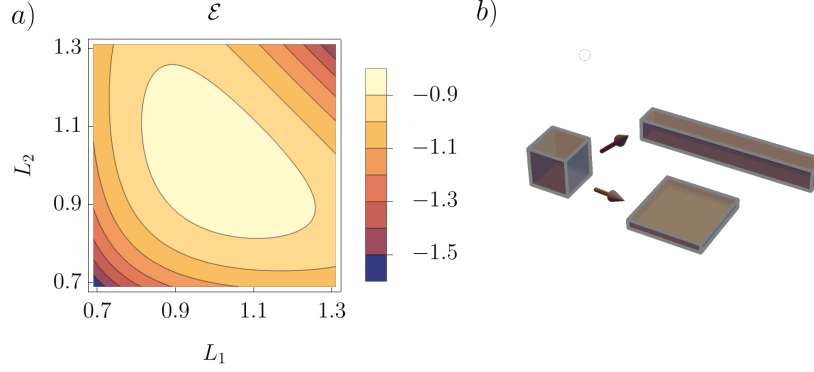


FIGURE 8. Total energy in a three-dimensional box with volume $V_{\Lambda} = L_1 L_2 L_3 = 1$, as a function of two sides L_1, L_2 , where the third side is fixed as $L_3 = 1/(L_1 L_2)$ (a). The energy is the lowest, when either two sides are small, or one side is small. The Casimir energy thus tends to deform cubes into either very long or very flat boxes (b).

where $\Lambda^* = \text{diag}(1/L_1, \dots, 1/L_d)$.

Consider the three-dimensional box with one short edge $L_1 = L \ll 1$ and two edges with unit length $L_2 = L_3 = 1$. The Casimir effect states, that there is a nonzero attractive force

$$F = -\frac{d\mathcal{E}}{dL} < 0$$

between the sides of the cube with unit length. Asymptotically it is known (see Ref [52]), that

$$F \approx -\frac{\pi^2}{30L^4}, \quad L \ll 1$$

which agrees with our numerics for small edge lengths. We further numerically determine the difference between the force in the sense of finite difference of the Epstein zeta function F_z and the asymptotic expression for the force F_{as} as defined above approximately equal to be

$$F_Z - F_{\text{as}} \approx -\frac{8\pi e^{-2\pi/L}}{L^3}$$

by a curve fit, see Figure 7.

The energy of a cube with unit volume $L_1 L_2 L_3 = 1$ is minimized by making either one or two edges small and the highest energy state is achieved by setting $L_1 = L_2 = L_3$, see Figure 8. Casimir force tends to deform cubes of fixed volume $L_1 L_2 L_3 = 1$ into either long or thin boxes, which agrees with the analysis in Ref [3].

In the massive case $m > 0$, the Casimir energy is no longer described by a lattice sum as in Definition 2.2, but the derivation of Crandall's representation can

still easily be adopted to yield an exponentially fast converging representation for the total energy. This highlights the strength of the method for the meromorphic continuation presented in this paper, which the authors will expand to even more general lattice sums in the future.

7. OUTLOOK AND CONCLUSIONS

The Epstein zeta function forms the basis for computing multidimensional lattice sums that appear in many physical systems of relevance, ranging from theoretical chemistry [40], over condensed matter physics [10, 5], to quantum field theory [3, 27]. This work, together with the implementation in `EpsteinLib`, solves the long-standing issue of efficiently computing the Epstein zeta function and makes it accessible as a powerful computational and exploratory tool. We expect that our theoretical analysis of the properties of the Epstein zeta function, in particular its singularities in all arguments, will allow for a unifying treatment of anomalous behavior in many systems with long-range interactions, both classical and quantum. We have demonstrated this for quantum spin systems with long-range interactions generalizing the results from Refs. [51, 36]. The regularised Epstein zeta function allows for the efficient computation of integrals involving the Epstein zeta function, as the singularity is analytically known and can be handled via specialized techniques like Duffy transformations [18], while the regularised zeta function is analytic in the first Brillouin zone and can be integrated using standard Gauss quadrature, with applications to unconventional superconductivity [10]. `EpsteinLib` is already actively being used by the quantum condensed matter community, see [34].

In future work, we will include the recent extension of Crandall’s formula to translationally non-invariant point sets in Ref. [7] in `EpsteinLib` as well as other generalized zeta functions. We plan to develop an algorithm for stably computing derivatives of the Epstein zeta function of arbitrary order in \mathbf{y} , which correspond to generalized lattice sums [9] that have direct applications in the Singular Euler-Maclaurin expansion [10]. We further plan to develop specialized algorithms for high-dimensional sums as well as expansions for lattice matrices with large condition numbers. Finally, we will study the efficient evaluation of Epstein zeta functions for complex exponents ν , which would open up the possibility for computational studies of non-trivial zeros of Epstein zeta functions.

ACKNOWLEDGEMENTS

We thank Torsten Keßler, Daniel Seibel, Kirill Serkh, Gary Schmiedinghoff, and Sergej Rjasanow for insightful comments and valuable discussions that helped improve this manuscript. We acknowledge our DevOps engineer Jan Schmitz for his significant contributions to the development of the library.

APPENDIX A. LATTICE SUMS

The following lemma proves absolute convergence of lattice sums for summands with sufficiently fast power-law decay. The idea of this proof can be found in [37, Lemma 3.14], who accredited the two-dimensional case to Weierstraß and the generalization to Eisenstein.

Lemma A.1. *Let $\Lambda = AZ^d$ with $A \in \mathbb{R}^{d \times d}$ regular, and $\nu \in \mathbb{C}$ with $\operatorname{Re}(\nu) > d$. Then, the lattice sum*

$$\sum'_{\mathbf{z} \in \Lambda} \frac{1}{|\mathbf{z}|^\nu}$$

converges absolutely.

Proof. First, recall that $|\mathbf{z}|^\nu = |\mathbf{z}|^s$ with $s = \operatorname{Re}(\nu)$. We now use the inequality

$$|A\mathbf{z}| \geq \|A^{-1}\|^{-1}|\mathbf{z}| = c|\mathbf{z}|$$

in order to bound the general lattice sum by a sum over \mathbb{Z}^d , yielding

$$\sum'_{\mathbf{z} \in \Lambda} \frac{1}{|\mathbf{z}|^s} \leq \frac{2^d}{c^s} \sum_{\mathbf{z} \in \mathbb{N}_0^d} \frac{1}{|\mathbf{z}|^s} = \frac{2^d}{c^s} \sum_{n=1}^d \binom{d}{n} \sum_{\mathbf{z} \in \mathbb{N}_+^n} \frac{1}{|\mathbf{z}|^s}$$

where the last equality is obtained by reordering the summands with respect to the number n of non-zero entries of \mathbf{z} . Therefore, we only need to show, that

$$\sum_{\mathbf{z} \in \mathbb{N}_+^n} \frac{1}{|\mathbf{z}|^s}$$

converges for $s > d$ and $1 \leq n \leq d$. Inserting the inequality of arithmetic and geometric means,

$$\frac{z_1^2 + \cdots + z_n^2}{n} \geq (z_1^2 z_2^2 \cdots z_n^2)^{1/n},$$

then yields

$$\sum_{\mathbf{z} \in \mathbb{N}_+^n} \frac{1}{|\mathbf{z}|^s} \leq n^{-s/2} \sum_{\mathbf{z} \in \mathbb{N}_+^n} (z_1 z_2 \cdots z_n)^{-s/n} = n^{-s/2} \zeta(s/n)^n,$$

where the series representation of the Riemann zeta function converges as $s/n \geq s/d > 1$. \square

APPENDIX B. PROPERTIES OF THE CRANDALL FUNCTIONS

For real exponents ν , the properties of the upper Crandall function are a direct consequence of the integral representation.

Lemma B.1. *Let $\nu \in \mathbb{R}$, $\mathbf{z} \in \mathbb{R}^d \setminus \{\mathbf{0}\}$. Then, the upper Crandall function $G_\nu(\cdot)$ is rotationally symmetric and globally decreasing in the norm of \mathbf{z} .*

Proof. Write $G_\nu(\mathbf{z})$ as

$$G_\nu(\mathbf{z}) = \int_{-1}^1 |t|^{-\nu} e^{-\pi \mathbf{z}^2 / t^2} \frac{dt}{t}$$

and note that the integrand is rotationally symmetric, positive, and strictly decreasing in \mathbf{z}^2 . The integral inherits these properties. \square

The radial symmetry of G allows to rewrite the integral in polar coordinates, reducing them to the one-dimensional case. The following lemma allows for their evaluation in terms of Crandall functions.

Lemma B.2. *Let $t \in \mathbb{R}$ and let $s \in \mathbb{R} \setminus \{t\}$. Then, for any $r > 0$, we have*

$$\int_r^\infty u^t G_s(u) \frac{du}{u} = r^t \frac{G_t(r) - G_s(r)}{t - s}.$$

Proof. After inserting the definition and substituting $\tilde{u} = \pi u^2$, we find

$$\int_r^\infty u^t G_s(u) \frac{du}{u} = \frac{1}{2\sqrt{\pi}^t} \int_{\pi r^2}^\infty \tilde{u}^{(t-s)/2} \Gamma(s/2, \tilde{u}) \frac{d\tilde{u}}{\tilde{u}}.$$

Notice that for any $a, v \in \mathbb{R}$, integration by parts yields

$$v \int_{r_0}^\infty \Gamma(a, u) u^{v-1} du = \Gamma(a + v, r_0) - r_0^v \Gamma(a, r_0),$$

for any $r_0 > 0$, where the boundary term vanishes due to the superpolynomial decay of $\Gamma(a, u)$ in u , as seen in the proof of Lemma 2.9. We thus obtain

$$\int_r^\infty u^t G_s(u) \frac{du}{u} = \frac{\Gamma(t/2, \pi r^2) - (\pi r^2)^{(t-s)/2} \Gamma(s/2, \pi r^2)}{\sqrt{\pi}^t (t - s)}.$$

Rewriting in terms of the upper Crandall function completes the proof. \square

The regularised Crandall function as defined in Theorem 2.15 is entire in \mathbf{z} for every fixed exponent $\nu \in \mathbb{C}$.

Lemma B.3. *Let $\nu \in \mathbb{C}$, let $d \in \mathbb{N}_+$ and let $\lambda > 0$. Then, $G_{\nu, \lambda}^{\text{reg}}(\mathbf{z})$ is holomorphic in $\mathbf{z} \in \mathbb{C}^d$.*

Proof. Assume $\nu \notin -2\mathbb{N}_0$, then $G_{\nu, \lambda}^{\text{reg}}(\mathbf{z})$ is holomorphic in $\mathbf{z} \in \mathbb{C}^d$ by Lemma 2.9 (1). Now, let $\nu = -2k$ for $k \in \mathbb{N}_0$ and

$$f_\lambda(w) = \frac{(-1)^k}{k!} (H_k - \gamma - \lambda^{2k} \log \lambda^2) w^k - \sum_{\substack{n=0 \\ n \neq k}}^\infty \frac{(-w)^n}{(n-k)n!}.$$

Since a power series is holomorphic if and only if it converges absolutely and

$$G_{\nu, \lambda}^{\text{reg}}(\mathbf{z}) = f_\lambda(\pi \mathbf{z}^2),$$

it suffices to show that

$$\sum_{\substack{n=0 \\ n \neq k}}^\infty \frac{(-w)^n}{(n-k)n!}$$

converges absolutely. The absolute value of the summands for $n \neq k$ is bounded by

$$\frac{|w|^n}{|n-k|n!} \leq \frac{|w|^n}{n!}$$

and thus, the exponential function is an absolute majorant of the power series associated with

$$\frac{(-1)^k}{k!} (H_k - \gamma - \lambda^{2k} \log \lambda^2) w^k - f_\lambda(w). \quad \square$$

APPENDIX C. TRUNCATION

For the investigation of the summation cutoff, it is sufficient to consider the lattice \mathbb{Z}^d , as the following lemma shows.

Lemma C.1. *Let $\Lambda = A\mathbb{Z}^d$ for $A \in \mathbb{R}^{d \times d}$ regular. Then, for any set $M \subset \mathbb{R}^d \setminus \{\mathbf{0}\}$, and $\mathbf{v} \in \mathbb{R}^d$, we have*

$$\sum_{\mathbf{z} \in \Lambda \cap M} G_\nu(c(\mathbf{z} + \mathbf{v})) \leq \sum_{\mathbf{z} \in \mathbb{Z}^d \cap A^{-1}M} G_\nu\left(\frac{c(\mathbf{z} + A^{-1}\mathbf{v})}{\|A^{-1}\|}\right),$$

with $\|\cdot\|$ the spectral norm.

Proof. The result follows directly from

$$|A(\mathbf{z} + A^{-1}\mathbf{v})| = \|A^{-1}\|^{-1}(\|A^{-1}\| \|A(\mathbf{z} + A^{-1}\mathbf{v})\|) \geq \|A^{-1}\|^{-1} |\mathbf{z} + A^{-1}\mathbf{v}|$$

as $G_\nu(\mathbf{z})$ is rotationally symmetric and strictly decreasing in the norm of \mathbf{z} , see Lemma B.1. \square

The following lemma allows us to bound the number of summands in shells with width $\varepsilon > 0$ in the multidimensional sums in Crandall's representation.

Lemma C.2. *Let $d \in \mathbb{N}_+$, let $r > 0$ and let*

$$N_d(r) = \sup_{\mathbf{v} \in \mathbb{R}^d} (\#\{\mathbf{z} \in \mathbb{Z}^d : |\mathbf{z} + \mathbf{v}| \leq r\}),$$

where the cardinality $\#$ denotes the number of elements in a set. Then, for any $r > \sqrt{d}$ and $0 < \varepsilon \leq (r - \sqrt{d})/2$, it holds that

$$N_d(r + \varepsilon) \leq \frac{(3/2)^d \pi^{d/2}}{\Gamma(d/2 + 1)} r^d.$$

Proof. Consider the disjoint union of hypercubes

$$V = \bigcup_{\substack{\mathbf{z} \in \mathbb{Z}^d + \mathbf{v} \\ |\mathbf{z}| < r + \varepsilon}} (\mathbf{z} + (-1/2, 1/2)^d).$$

Then $N_d(r + \varepsilon) = \text{Vol } V$. Since the maximum distance of any $\mathbf{z} \in \mathbb{R}^d$ to the nearest point in $\mathbb{Z}^d + \mathbf{v}$ is $\sqrt{d}/2$, we obtain

$$V \subset \overline{B_{\tilde{r}}}(\mathbf{0}).$$

with $\tilde{r} = r + \varepsilon + \sqrt{d}/2$, from which the bound

$$N_d(r + \varepsilon) \leq \text{Vol}(\overline{B_{\tilde{r}}}(\mathbf{0})) = \frac{\pi^{d/2} \tilde{r}^d}{\Gamma(d/2 + 1)}$$

follows. The desired estimate is then obtained from the inequality $\varepsilon + \sqrt{d}/2 \leq r/2$, as then $\tilde{r} \leq 3r/2$. \square

We present the proof for the rigorous error bound in Crandall's representation.

Proof of Theorem 3.3. By Lemma C.1 the absolute value of the remainder is bounded by

$$\frac{\pi^{\nu/2}}{|\Gamma(\nu/2)|} \left[\sum_{\substack{\mathbf{z} \in \mathbb{Z}^d \\ |\mathbf{z} - A^{-1}\mathbf{x}| > r/\|A\|}} G_\nu\left(\frac{\mathbf{z} - A^{-1}\mathbf{x}}{\|A^{-1}\|}\right) + \frac{1}{V_\Lambda} \sum_{\substack{\mathbf{k} \in \mathbb{Z}^d \\ |\mathbf{k} + A^T\mathbf{y}| > r/\|A^{-1}\|}} G_{d-\nu}\left(\frac{\mathbf{k} + A^T\mathbf{y}}{\|A\|}\right) \right]$$

where we enlarged the summation range using $A^{-1}(\mathbb{R}^d \setminus B_r) \subseteq \mathbb{R}^d \setminus B_{r/\|A\|}$ and $A^T(\mathbb{R}^d \setminus B_r) \subseteq \mathbb{R}^d \setminus B_{r/\|A^{-T}\|}$ with $\|A^{-T}\| = \|A^{-1}\|$.

We now subdivide the sums into sums over spherical shells of width $\varepsilon' > 0$ as follows

$$\sum_{\substack{\mathbf{k} \in \mathbb{Z}^d \\ |\mathbf{k} + \mathbf{v}| > r'}} G_s(c(\mathbf{k} + \mathbf{v})) = \sum_{n=0}^{\infty} \sum_{\substack{\mathbf{k} \in \mathbb{Z}^d \\ |\mathbf{k} + \mathbf{v}| > r' + n\varepsilon' \\ |\mathbf{k} + \mathbf{v}| \leq r' + (n+1)\varepsilon'}} G_s(c(\mathbf{k} + \mathbf{v}))$$

for $r', c > 0$, $\mathbf{v} \in \mathbb{R}^d$, and $s \in \mathbb{C}$. We then use the strict monotonic decrease and rotational symmetry of $G_s(\cdot)$ to bound the value of G_s by its maximum within the shell. We further bound the number of lattice points within the shell by the number of points within the closed ball of radius $r' + (n+1)\varepsilon'$, with the bound provided in Lemma C.2. We obtain for $0 < \varepsilon' \leq (r' - \sqrt{d})/2$,

$$\sum_{\substack{\mathbf{k} \in \mathbb{Z}^d \\ |\mathbf{k} + \mathbf{v}| > r'}} G_s(c(\mathbf{k} + \mathbf{v})) \leq C \sum_{n=0}^{\infty} (r' + n\varepsilon')^d G_s(c(r' + n\varepsilon')),$$

with $C = (3/2)^d \pi^{d/2} / \Gamma(d/2 + 1)$. By monotonicity, this expression is bounded by the associated integral

$$C \int_{-1}^{\infty} (r' + n\varepsilon')^d G_s(c(r' + n\varepsilon')) dn.$$

Applying Lemma B.2, we find

$$C \frac{1}{\varepsilon'} \left[(r' - \varepsilon')^{d+1} \frac{G_{d+1}(c(r' - \varepsilon')) - G_s(c(r' - \varepsilon'))}{d + 1 - s} \right]$$

where the limit $s \rightarrow d + 1$ is well-defined, since $G_s(u)$, $u > 0$, is holomorphic in $s \in \mathbb{C}$ by Lemma 2.9. Letting $r' = r/\|A\|$, $c = 1/\|A^{-1}\|$ for the first sum, and $r' = r/\|A^{-1}\|$, $c = 1/\|A\|$ as well as $\tilde{\varepsilon} = c\varepsilon'$ leads to the bound

$$\kappa(A)^{d+1} C \frac{1}{\tilde{\varepsilon}} \left[\left(\frac{r}{\kappa(A)} \right)^{d+1} \frac{G_{d+1}(r/\kappa(A) - \tilde{\varepsilon}) - G_s(r/\kappa(A) - \tilde{\varepsilon})}{d + 1 - s} \right]$$

where we used that $c \leq 1$ since both $\|A\| \geq 1$ and $\|A^{-1}\| \geq 1$ due to $\det(A) = 1$. The bound above holds for every

$$0 < \tilde{\varepsilon} \leq (r/\kappa(A) - \sqrt{d}) / \max\{\|A\|, \|A^{-1}\|\} / 2.$$

The right-hand side of the expression above is, by the constraint on r , larger than ε . Thus, we may choose $\tilde{\varepsilon} = \varepsilon$. Including the ν -dependent prefactor yields the statement. \square

REFERENCES

- [1] Rémy Abergel and Lionel Moisan. “Algorithm 1006: Fast and Accurate Evaluation of a Generalized Incomplete Gamma Function”. In: *ACM Trans. Math. Softw.* 46.1 (Mar. 2020). ISSN: 0098-3500. DOI: 10.1145/3365983. URL: <https://doi.org/10.1145/3365983>.
- [2] M. Abramowitz and I.A. Stegun. *Handbook of Mathematical Functions with Formulas, Graphs, and Mathematical Tables*. Applied mathematics series. U.S. Government Printing Office, 1964. URL: <https://books.google.de/books?id=3X55fTnM848C>.

- [3] Jan Ambjørn and Stephen Wolfram. “Properties of the Vacuum. I. Mechanical and Thermodynamic”. In: *Annals of Physics* 147.1 (Aug. 1983), pp. 1–32. ISSN: 00034916. DOI: 10.1016/0003-4916(83)90065-9. (Visited on 05/23/2024).
- [4] Jean-Paul Berrut and Lloyd N. Trefethen. “Barycentric Lagrange Interpolation”. In: *SIAM Review* 46.3 (Jan. 2004), pp. 501–517. ISSN: 0036-1445, 1095-7200. DOI: 10.1137/S0036144502417715. (Visited on 11/22/2024).
- [5] J. Borwein et al. *Lattice Sums Then and Now*. Encyclopedia of Mathematics and its Applications. Cambridge University Press, 2013. URL: <https://doi.org/10.1017/CB09781139626804>.
- [6] Jonathan M Borwein, O-Yeat Chan, et al. “Uniform bounds for the complementary incomplete gamma function”. In: *Mathematical Inequalities and Applications* 12 (2009), pp. 115–121.
- [7] Andreas Buchheit, Torsten Keßler, and Kirill Serkh. “On the Computation of Lattice Sums without Translational Invariance”. In: *Mathematics of Computation* (Oct. 2024). ISSN: 0025-5718, 1088-6842. DOI: 10.1090/mcom/4024. (Visited on 10/30/2024).
- [8] Andreas A Buchheit and Torsten Keßler. “On the Efficient Computation of Large Scale Singular Sums with Applications to Long-Range Forces in Crystal Lattices”. In: *J. Sci. Comput.* 90.1 (2022), pp. 1–20. DOI: 10.1007/s10915-021-01731-5. URL: <https://doi.org/10.1007/s10915-021-01731-5>.
- [9] Andreas A Buchheit and Torsten Keßler. “Singular Euler–Maclaurin expansion on multidimensional lattices”. In: *Nonlinearity* 35.7 (2022), p. 3706.
- [10] Andreas A. Buchheit et al. “Exact continuum representation of long-range interacting systems and emerging exotic phases in unconventional superconductors”. In: *Phys. Rev. Res.* 5 (4 Oct. 2023), p. 043065. DOI: 10.1103/PhysRevResearch.5.043065. URL: <https://link.aps.org/doi/10.1103/PhysRevResearch.5.043065>.
- [11] Antony Burrows, Shaun Cooper, and P. Schwerdtfeger. “The Madelung Constant in N Dimensions”. In: *Proceedings of the Royal Society A: Mathematical, Physical and Engineering Sciences* 478.2267 (Nov. 2022), p. 20220334. ISSN: 1364-5021, 1471-2946. DOI: 10.1098/rspa.2022.0334. (Visited on 05/23/2024).
- [12] Antony Burrows, Shaun Cooper, and Peter Schwerdtfeger. “Lattice Sum for a Hexagonal Close-Packed Structure and Its Dependence on the c/a Ratio of the Hexagonal Cell Parameters”. In: *Physical Review E* 107.6 (June 2023). ISSN: 2470-0045, 2470-0053. DOI: 10.1103/physreve.107.065302. (Visited on 09/17/2024).
- [13] Hendrik BG Casimir. “On the attraction between two perfectly conducting plates”. In: *Indag. Math.* 10.4 (1948), pp. 261–263.
- [14] Hendrik BG Casimir and Dirk Polder. “The influence of retardation on the London-van der Waals forces”. In: *Physical Review* 73.4 (1948), p. 360. URL: <https://doi.org/10.1103/PhysRev.73.360>.
- [15] Sarvadaman Chowla and Atle Selberg. “On Epstein’s zeta function (I)”. In: *Proceedings of the National Academy of Sciences* 35.7 (1949), pp. 371–374. URL: <https://doi.org/10.1073/pnas.35.7.371>.
- [16] R. Crandall. “Unified algorithms for polylogarithm, L-series, and zeta variants”. In: *Algorithmic Reflections: Selected Works*. PSIPress, 2012.

- [17] *NIST Digital Library of Mathematical Functions*. <https://dlmf.nist.gov/>, Release 1.2.0 of 2024-03-15. F. W. J. Olver, A. B. Olde Daalhuis, D. W. Lozier, B. I. Schneider, R. F. Boisvert, C. W. Clark, B. R. Miller, B. V. Saunders, H. S. Cohl, and M. A. McClain, eds. URL: <https://dlmf.nist.gov/>.
- [18] M. G. Duffy. “Quadrature over a pyramid or cube of integrands with a singularity at a vertex”. In: *SIAM J. Numer. Anal.* 19.6 (1982), pp. 1260–1262. URL: <https://doi.org/10.1137/0719090>.
- [19] Ariel Edery. “Multidimensional Cut-off Technique, Odd-Dimensional Epstein Zeta Functions and Casimir Energy of Massless Scalar Fields”. In: (2005). DOI: 10.48550/ARXIV.MATH-PH/0510056. (Visited on 05/14/2024).
- [20] E Elizalde. “Multidimensional extension of the generalized Chowla–Selberg formula”. In: *Communications in mathematical physics* 198.1 (1998), pp. 83–95.
- [21] O. Emersleben. “Zetafunktionen und elektrostatische Gitterpotentiale. I”. In: *Phys. Z* 24 (1923), pp. 73–80.
- [22] O. Emersleben. “Zetafunktionen und elektrostatische Gitterpotentiale. II”. In: *Phys. Z* 24 (1923), pp. 97–104.
- [23] P. Epstein. “Zur Theorie allgemeiner Zetafunktionen”. In: *Math. Ann.* 56 (1903), pp. 615–644. URL: <https://doi.org/10.1007/BF01444309>.
- [24] P. Epstein. “Zur Theorie allgemeiner Zetafunktionen. II”. In: *Math. Ann.* 63 (1906), pp. 205–216. URL: <https://doi.org/10.1007/BF01449900>.
- [25] Walter Gautschi. “A Computational Procedure for Incomplete Gamma Functions”. In: *ACM Trans. Math. Softw.* 5 (1979), pp. 466–481.
- [26] Amparo Gil, Javier Segura, and Nico M Temme. “Efficient and accurate algorithms for the computation and inversion of the incomplete gamma function ratios”. In: *SIAM Journal on Scientific Computing* 34.6 (2012), A2965–A2981.
- [27] Stephen W Hawking. “Zeta function regularization of path integrals in curved spacetime”. In: *Communications in Mathematical Physics* 55 (1977), pp. 133–148. URL: <https://doi.org/10.1007/BF01626516>.
- [28] L. Hörmander. *The Analysis of Linear Partial Differential Operators I: Distribution Theory and Fourier Analysis*. Classics in Mathematics. Springer, 2003.
- [29] Lars Hörmander. *An Introduction to Complex Analysis in Several Variables*. 3rd ed. rev. North-Holland Mathematical Library 07. Amsterdam New York Oxford: North-Holland, 1990. ISBN: 978-0-444-88446-6.
- [30] F. Johansson. “Arb: efficient arbitrary-precision midpoint-radius interval arithmetic”. In: *IEEE Transactions on Computers* 66 (8 2017), pp. 1281–1292. DOI: 10.1109/TC.2017.2690633.
- [31] Fredrik Johansson. “Arb: Efficient Arbitrary-Precision Midpoint-Radius Interval Arithmetic”. In: *IEEE Transactions on Computers* 66.8 (2017), pp. 1281–1292. DOI: 10.1109/TC.2017.2690633.
- [32] W. Kahan. “Pracniques: further remarks on reducing truncation errors”. In: *Commun. ACM* 8.1 (Jan. 1965), p. 40. ISSN: 0001-0782. DOI: 10.1145/363707.363723. URL: <https://doi.org/10.1145/363707.363723>.
- [33] Haseo Ki. “All but finitely many non-trivial zeros of the approximations of the Epstein zeta function are simple and on the critical line”. In: *Proceedings of the London Mathematical Society* 90.2 (2005), pp. 321–344.

- [34] Jan Alexander Koziol, Giovanna Morigi, and Kai Phillip Schmidt. “Quantum phases of hardcore bosons with repulsive dipolar density-density interactions on two-dimensional lattices”. In: *arXiv preprint arXiv:2311.10632, accepted in SciPost Physics* (2023). URL: <https://doi.org/10.48550/arXiv.2311.10632>.
- [35] Xin-zhou Li et al. “Attractive or Repulsive Nature of the Casimir Force for Rectangular Cavity”. In: *Physical Review D* 56.4 (Aug. 1997), pp. 2155–2162. ISSN: 0556-2821, 1089-4918. DOI: 10.1103/PhysRevD.56.2155. (Visited on 05/16/2024).
- [36] D. Peter et al. “Anomalous behavior of spin systems with dipolar interactions”. In: *Phys. Rev. Lett.* 109.2 (2012), p. 025303. URL: <https://doi.org/10.1103/PhysRevLett.109.025303>.
- [37] Reinhold Remmert and Georg Schumacher. *Funktionentheorie 2*. Heidelberg: Springer Berlin, 2007. ISBN: 978-3-540-40432-3.
- [38] Alejandro W Rodriguez, Federico Capasso, and Steven G Johnson. “The Casimir effect in microstructured geometries”. In: *Nature photonics* 5.4 (2011), pp. 211–221. URL: <https://doi.org/10.1038/nphoton.2011.39>.
- [39] Walter Rudin. *Real and complex analysis, 3rd ed.* USA: McGraw-Hill, Inc., 1987. ISBN: 0070542341.
- [40] Peter Schwerdtfeger and David J. Wales. “100 Years of the Lennard-Jones Potential”. In: *Journal of Chemical Theory and Computation* 20.9 (May 2024), pp. 3379–3405. ISSN: 1549-9618, 1549-9626. DOI: 10.1021/acs.jctc.4c00135. (Visited on 05/16/2024).
- [41] Daniel Shanks. “Calculation and Applications of Epstein Zeta Functions”. In: *Mathematics of Computation* 29.129 (1975), pp. 271–287. ISSN: 0025-5718, 1088-6842. DOI: 10.1090/S0025-5718-1975-0409357-2. (Visited on 07/17/2024).
- [42] Harold M Stark. “On the zeros of Epstein’s zeta function”. In: *Mathematika* 14.1 (1967), pp. 47–55.
- [43] E. M. Stein and G. Weiss. *Introduction to Fourier Analysis on Euclidean Spaces*. Princeton University Press, 1972.
- [44] Nico Temme. “On the computation of the incomplete gamma functions for large values of the parameters”. In: 1985. URL: <https://api.semanticscholar.org/CorpusID:261763729>.
- [45] Nico Temme. “Uniform asymptotic expansions of the incomplete gamma functions and the incomplete beta function”. In: *Mathematics of Computation* 29 (1975).
- [46] Audrey A. Terras. “Bessel Series Expansions of the Epstein Zeta Function and the Functional Equation”. In: *Transactions of the American Mathematical Society* 183 (1973), pp. 477–486. ISSN: 00029947. URL: <http://www.jstor.org/stable/1996480> (visited on 07/16/2024).
- [47] Francesco Giacomo Tricomi. “Sulla funzione gamma incompleta”. In: *Annali di Matematica Pura ed Applicata* 31 (1950), pp. 263–279. URL: <https://api.semanticscholar.org/CorpusID:120404791>.
- [48] H.S. Wall. *Analytic Theory of Continued Fractions*. Dover Books on Mathematics. Dover Publications, 1948. ISBN: 9780486830445. URL: <https://books.google.de/books?id=86ReDwAAQBAJ>.

- [49] D. Wolf et al. “Exact method for the simulation of Coulombic systems by spherically truncated, pairwise r^{-1} summation”. In: *J. Chem. Phys.* 110.17 (1999), pp. 8254–8282. URL: <https://doi.org/10.1063/1.478738>.
- [50] Bawei Wu and Per-Gunnar Martinsson. “Corrected trapezoidal rules for boundary integral equations in three dimensions”. In: *Numerische Mathematik* 149 (2021), pp. 1025–1071.
- [51] E. Yusuf, A. Joshi, and K. Yang. “Spin waves in antiferromagnetic spin chains with long-range interactions”. In: *Phys. Rev. B: Condens. Matter* 69.14 (2004), p. 144412. URL: <https://doi.org/10.1103/PhysRevB.69.144412>.
- [52] Eberhard Zeidler. *Quantum Field Theory I: Basics in Mathematics and Physics*. Berlin, Heidelberg: Springer Berlin Heidelberg, 2006. ISBN: 978-3-540-34762-0 978-3-540-34764-4. DOI: 10.1007/978-3-540-34764-4. (Visited on 05/10/2024).
- [53] Yichi Zhang et al. “Magnetic-field tuning of the Casimir force”. In: *Nature Physics* (2024), pp. 1–6. URL: <https://doi.org/10.1038/s41567-024-02521-0>.
- [54] Rongkuo Zhao et al. “Stable Casimir equilibria and quantum trapping”. In: *Science* 364.6444 (2019), pp. 984–987. URL: <https://doi.org/10.1126/science.aax0916>.
- [55] I.J. Zucker. “The Exact Evaluation of Some New Lattice Sums”. In: *Symmetry* 9.12 (2017), p. 314. URL: <https://doi.org/10.3390/sym9120314>.